

**REPORT DOCUMENTATION PAGE**Form Approved  
OMB No. 0704-0188

Public reporting burden for this collection of information is estimated to average 1 hour per response, including the time for reviewing instructions, searching existing data sources, gathering and maintaining the data needed, and completing and reviewing this collection of information. Send comments regarding this burden estimate or any other aspect of this collection of information, including suggestions for reducing this burden to Department of Defense, Washington Headquarters Services, Directorate for Information Operations and Reports (0704-0188), 1215 Jefferson Davis Highway, Suite 1204, Arlington, VA 22202-4302. Respondents should be aware that notwithstanding any other provision of law, no person shall be subject to any penalty for failing to comply with a collection of information if it does not display a currently valid OMB control number. **PLEASE DO NOT RETURN YOUR FORM TO THE ABOVE ADDRESS.**

<b>1. REPORT DATE (DD-MM-YYYY)</b> 28-07-2003		<b>2. REPORT TYPE</b> Final Technical Report		<b>3. DATES COVERED (From - To)</b> 01 May 2000 – 30 April 2003	
<b>4. TITLE AND SUBTITLE</b> Lifetime and Longevity of an Intense, Photoconductively-Switched Stacked Blumlein Modulator for Ultra-Wideband HPM Applications				<b>5a. CONTRACT NUMBER</b>	
				<b>5b. GRANT NUMBER</b> F49620-00-1-0296	
				<b>5c. PROGRAM ELEMENT NUMBER</b>	
<b>6. AUTHOR(S)</b> Carl B. Collins Farzin Davanloo				<b>5d. PROJECT NUMBER</b>	
				<b>5e. TASK NUMBER</b>	
				<b>5f. WORK UNIT NUMBER</b>	
<b>7. PERFORMING ORGANIZATION NAME(S) AND ADDRESS(ES)</b>  The University of Texas at Dallas 2601 North Floyd Road P.O. Box 830688 Richardson, Texas 75083-0688				<b>8. PERFORMING ORGANIZATION REPORT NUMBER</b>	
<b>9. SPONSORING / MONITORING AGENCY NAME(S) AND ADDRESS(ES)</b> Air Force Office of Scientific Research AFOSR/NE 4015 Wilson Blvd., Room 713 Arlington, VA 22203-1954				<b>10. SPONSOR/MONITOR'S ACRONYM(S)</b>	
				<b>11. SPONSOR/MONITOR'S REPORT NUMBER(S)</b>	
<b>12. DISTRIBUTION / AVAILABILITY STATEMENT</b>  Approved for public release; distribution unlimited					
<b>13. SUPPLEMENTARY NOTES</b>					
<b>14. ABSTRACT</b> In this work, experiments with the stacked Blumlein prototype pulsed were conducted under different conditions of operation at power levels bypassing 100 MW. Special attention was placed on broadening of the current channels in the avalanche photoconductive switch in order to improve lifetime. The mechanical and semiconductor properties of amorphous diamond were employed to improve the lifetime by coating the switch cathode or anode areas or both. Issues concerning the switch longevity were studied by fabrication and testing the GaAs photoconductive switches treated with the amorphous diamond under different switch configuration, gap settings, and diamond coating thickness. When the switch cathode was coated, the tunneling of electrons from amorphous diamond to GaAs provided pre-avalanche sites that diffused conduction current upon switch activation. On the other hand, the diamond coating of the switch anode resulted in increased hold-off characteristics and longer switch lifetimes by blocking leakage current during off-state stage of operation. A significant improvement in switch lifetime was demonstrated by coating the cathode and anode areas of a GaAs photoconductive switch with amorphous diamond and testing its performance in a high power operation with a prototype stacked Blumlein pulsed. In addition, elementary processes involved in conduction of a diamond-treated photoconductive switch were extensively examined.					
<b>15. SUBJECT TERMS</b> Stacked Blumlein Pulsers, Amorphous Diamond, High Gain GaAs Photoconductive Semiconductor Switch, Photoconductive Switching, High Power Repetitive Pulsers, Rectifying Heterojunction, Ultra-Wideband Applications					
<b>16. SECURITY CLASSIFICATION OF:</b> Unclassified			<b>17. LIMITATION OF ABSTRACT</b>  SAR	<b>18. NUMBER OF PAGES</b>  59	<b>19a. NAME OF RESPONSIBLE PERSON</b> Farzin Davanloo
<b>a. REPORT</b> U	<b>b. ABSTRACT</b> U	<b>c. THIS PAGE</b> U			<b>19b. TELEPHONE NUMBER (include area code)</b> (972)883-2863

20030910 016

## **Final Technical Report**

describing

Research for U.S. Air Force Office of Scientific Research (AFOSR)

entitled

**"Lifetime and Longevity of an Intense, Photoconductively - Switched Stacked Blumlein  
Modulator for Ultra - Wideband HPM Applications"**

for the period

**5/1/00 through 4/30/03**

**Grant No: F49620-00-1-0296**

Principal Investigators:

C. B. Collins

F. Davanloo

Center for Quantum Electronics  
University of Texas at Dallas  
P.O. Box 830688, Richardson, TX 75083-0688

## TABLE OF CONTENTS

INTRODUCTION.....	3
BLUMLEIN PULSERS.....	5
Devices Commutated by Conventional Switches.....	5
Photoconductively-Switched Stacked Blumlein Pulsers.....	10
High Gain Photoconductive Switch and Current Filamentation.....	15
AMORPHIC DIAMOND TREATMENT OF PHOTOCONDUCTIVE SWITCHES.....	18
Amorphic Diamond Deposition and General Properties.....	18
Heterojunction Devices Formed by Amorphic Diamond.....	21
Diamond Coated Photoconductive Switch.....	29
Junction Conduction Mechanism.....	35
Switch Behavior with Diamond Coating.....	39
SWITCH LIFETIME STUDIES.....	42
CONCLUSIONS.....	48
EXECUTIVE SUMMARY.....	50
Summary of the Results.....	50
Personnel Participated.....	51
Publications Resulted from this Work.....	52
RESEARCH SIGNIFICANCE AND POTENTIAL APPLICATIONS.....	53
REFERENCES.....	56

## INTRODUCTION

To fulfill the demand for pulsed power sources producing several hundred kV pulses at moderately high repetition rates, the University of Texas at Dallas (UTD) first introduced and implemented a new approach to combine the functions of pulse shaping and voltage multiplication using stacked Blumleins. This yielded the development of pulsers that consisted of several triaxial Blumleins stacked in series at one end. The lines were charged in parallel and synchronously commutated with a single switch at the other end. This allowed switching to take place at a low charging voltage relative to the pulser output voltage [1-4].

The stacked Blumlein pulsers have produced high power waveforms with pulse durations, risetimes and repetition rates in the range of 5-600 ns, 3-50 ns, and 1-1000 Hz, respectively using a thyatron or spark gap [1-4]. To generate waveforms with sub-nanosecond risetimes at high repetition rates, photoconductive switches offer significant advantages. Our recent efforts at UTD, for the first time, resulted in implementation and demonstration of several high power stacked Blumlein pulsers commutated by a single photoconductive switch. These devices have a compact geometry and are commutated by a GaAs photoconductive semiconductor switch (PCSS) triggered by a low power laser diode array [5-7].

Filamentation of the conductivity associated with high gain GaAs switches produces such high current density that the switches are damaged near the metal-semiconductor interface and the lifetime is limited. The semiconductor properties of amorphous diamond, also developed at UTD, have been employed to improve the PCSS longevity by coating the switch cathode or anode areas or both. For example if the switch cathode is coated, the tunneling of electrons from amorphous diamond to GaAs during the off-state stage of PCSS operation provides pre-avalanche sites that diffuse conduction current upon switch activation. A significant improvement in



switch lifetime has been demonstrated by testing the diamond-coated switch performance in a stacked Blumlein prototype.

Pulsed power systems to drive Ultra-Wideband (UWB) sources require the ability to provide fast rising pulses for driving antennas at high voltages [8]. These have been usually limited to the order of 10 kV in the array photoconductive semiconductor switched sources built to date. The product of the field strength times the range is the performance criterion that is used to rate performance of a combination pulser and antenna. The goal is to develop UWB sources in terms that provide sufficient field strength at a given range. The limitation in existing technologies is switch voltage with acceptable switch lifetime. The opposing trend in switch voltage and switch lifetime makes it undesirable simply to operate the switches at higher voltages, as switch lifetime drops dramatically with increased operating voltage.

The work described in this report is the progress toward developing a technology in pulsed power that can increase the voltage delivered to UWB antennas with reasonable switch lifetimes. Advances in stacked Blumlein technology for voltage multiplication at UTD, together with the results obtained in this study, offer exciting possibilities for a variety of HPM applications especially in array UWB and compact UWB sources. With power levels approaching 150 MW, broad-band HPM sources operating at kilohertz repetition rates can be conceived that match characteristic impedance of the compact stacked Blumlein pulsers to intrinsic impedance of free space through special purpose antenna interfaces.

## BLUMLEIN PULSERS

### 1. Devices Commutated by Conventional Switches

A major step in the development of intense pulsed power supplies with the elimination of the output switch, the element which most critically limits the repetition rate of firing was reported by our group [9]. Developed to power pulsed x-ray diode for the excitation of nuclear fluorescence, we succeeded in switching a  $1\ \Omega$  Blumlein with a hydrogen thyratron at a repetition rate of 100 Hz. Higher average x-ray powers were obtained both by scaling these devices in size and by operating them at higher charging voltages [10]. The spectral content of the fluxes emitted by different anodes was measured reliably. A third of the energy was found to be in K lines. The remainder was distributed over a fairly broad band of true continua with the endpoint energy lying above the charging voltage of the Blumlein circuit. The combination of all aspects in the development of these devices resulted in an x-ray source with an energy range that spanned from 5 to 100 keV. Operating parameters for these single Blumlein pulse power devices were constrained by the limitation on peak currents and the voltage tolerances of existing commercial thyratrons.

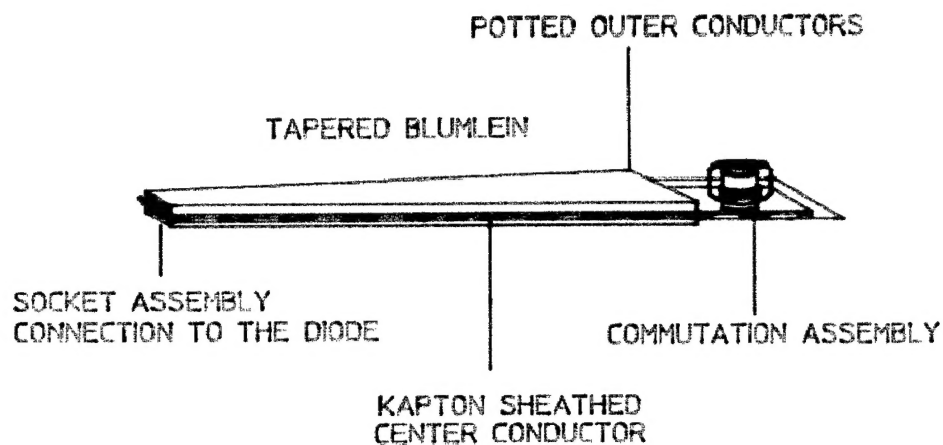
To access higher voltages, we reported construction and characterization of a laboratory scale pulse generator, driven by stacked Blumleins [11]. It had eight Blumleins which were charged in parallel at one end and switched with a single thyratron. Scaling of such an impulsive device to potentials exceeding 400 kV, while retaining the capabilities for operation at high-repetition rates was reported subsequently [12]. There a second prototype pulse x-ray generator, driven by stacked Blumleins was described. An extensive characterization of the performance of this pulse power device was given. Improvements in the design and construction of this device

resulted in better voltage gains and it was noted that the maximum number of lines that can be stacked had not been reached. An x-ray diode matched to this power source produced intense x-ray pulses containing useful fluxes of photons having energies up to 300 keV [12].

Design and construction of the pulse forming system for these Blumlein generators commutated with conventional switches, have been given elsewhere [1-5, 9-12]. Briefly, a single Blumlein pulse generator consisted of two critical subassemblies: (1) a single Blumlein pulse forming line, and (2) a commutation system capable of operation at high repetition rates. The basic organization is shown schematically in Fig. 1 (a). The Blumleins were constructed from copper plates, potted with epoxy on outer surfaces to reduce corona, and separated by laminated layered Kapton (polyimide) dielectrics. Scaling of these devices was studied by construction of several systems with different lengths, capacitances, and impedances [9]. All Blumleins had a smooth taper that increased from the load diode end to the thyatron switching end as seen in Fig. 1 (a).

In operation, the middle conductor was charged to a positive high voltage that could be varied to 75 kV, and commutation was affected by a hydrogen thyatron or a spark gap. Different types of thyatrons and spark gaps with different voltage hold off characteristics were used. This resulted in peak voltages available at the load which spanned the range from 5 to 100 kV. To access voltages far above 100 kV, a stacked Blumlein pulse generator was designed and constructed [1-5, 11-12]. It consisted of three separate but integrated subassemblies: (1) the switching assembly, (2) pulse forming Blumleins, and (3) the pulse stacking module. The basic organization for the second prototype stack Blumlein pulse generator with twelve Blumlein lines is shown in Fig. 1 (b).

a)



b)

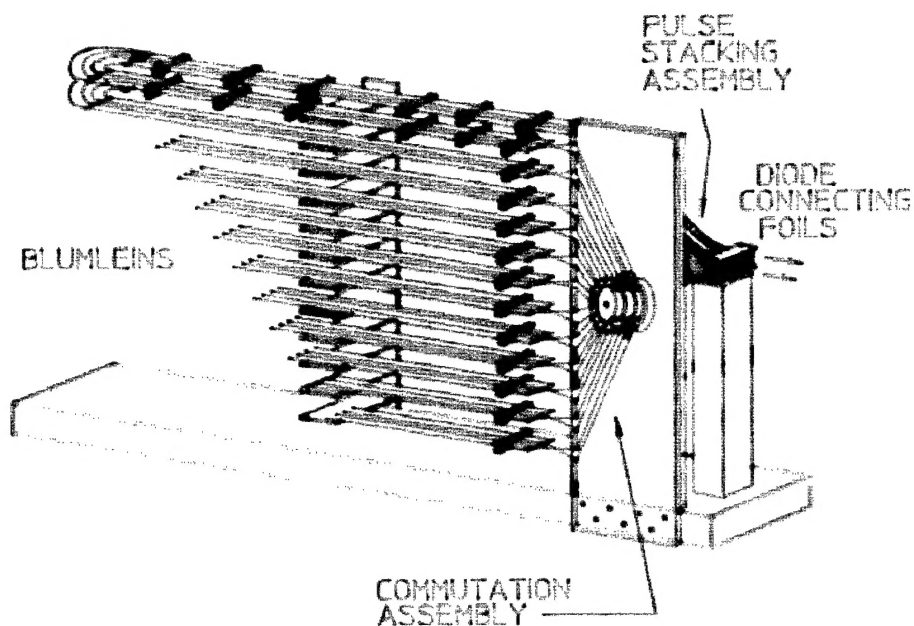


**Figure 1.** Schematic drawings of the high repetition rate, Blumlein pulse power generators developed at University of Texas at Dallas. (a) Pulse generator with a single traxial Blumlein pulse forming line. (b) Pulse generator with several Blumlein modules connected in parallel at switching end and stacked in series across the load diode.

Extensive characterization of this prototype pulse generator with eight lines has been performed [11]. Simulation studies of voltage and current profiles showed that the distribution of the switched current among the Blumleins played an important role in system voltage gain. Blumleins were connected to the thyatron through several current distribution schemes. To increase the voltage gain at the stacking module, the number of Blumleins were increased to twelve. Distortions of the Propagated pulses were minimized by directly connecting the lines to the thyatron as seen in Fig. 1 (b).

The ground plate from each line was connected to the thyatron cathode mounting ring and twelve individual current returns connected the high voltage plates of the lines to the thyatron anode. These current return legs, with the same width as the lines were arranged coaxially around the thyatron. The assembly was pressed by two sheets of plexiglass. Grooves were machined into the plates the same size and depth as the copper plates, 2.5 cm wide and 0.32 cm deep. The sheets of plastic were then bolted together, forming both the mount and press system for the commutation unit. Blumlein ground copper plates connecting to the thyatron cathode, were separated from the high voltage plates by laminated Kapton insulators. Blumlein high voltage plates were connected to the thyatron anode through coaxial current returns. These components were kept together by two bolted grooved sheets of plexiglass as shown in Fig. 1(b). The use of a single switching element allowed the device to be operated at repetition rates to 300 Hz.

The commutation assembly was mounted in a vertical plane while the lines were set on horizontal shelves. Copper foils and Kapton (Polyimide) dielectric insulators were smoothly twisted to connect the thyatron assembly to the Blumleins. Care was taken to maintain a constant impedance throughout the twist. The pulse forming lines were constructed from 3.7 m long sections of copper plate. They were 3.2 mm thick and 2.5 cm wide with rounded edges.

Two 2.3 mm thick Kapton insulator plates were placed along the length between the copper conductors. The dielectric sheets were 15.2 cm wide to prevent electrical breakdown between copper lines. This assembly was held together by delrin plastic presses. They were installed and tightened around the lines at 30 cm intervals. Two of these sections were set on each shelf and a carefully fabricated u-turn was used to connect them together. In this way twelve Blumleins in the shape of a "U," each with a length of 8.2 m, were placed on the shelves, one above the other. At one end, these lines were connected to the vertical thyatron assembly, and at the other end, the lines were stacked in series behind the thyatron mounting assembly, as seen in Fig. 1 (b). The Kapton insulators were constructed from thirteen 0.127 mm thick Kapton sheets. They were laminated together with a high dielectric epoxy. The thickness of these boards varied by less than 10% over their entire length. This construction procedure resulted in an impedance of  $40\ \Omega$  for each Blumlein.

For the performances described here commutation was affected by a three-stage EG&G hydrogen thyatron mounted in a grounded cathode configuration. This type of thyatron was capable of switching peak forward currents of 20 kA in tens of nanoseconds. However, it could not carry peak inverse currents in excess of 1.5 kA without sustaining severe damage. Special care was given to the load matching conditions in order to avoid voltage oscillations that could generate un-acceptable reverse currents. The capacitances of the Blumleins were altered to reduce the magnitude of the current pulse at the thyatron. The amount of switched charge was controlled by discontinuing the high voltage plates of each line at a certain length from the thyatron. Thus, the voltages developed across the triplate Blumleins were transferred to the biaxial transmission lines that in turn, were stacked on each other in the series connection. Copper foils were connected to the ends of the lines and angled together, along with the

dielectric, to stack directly on top of one another. The lines were then connected in series for about 10 cm before the anode and cathode leads from the load diode inserted into the stack.

In operation, both the single and stacked Blumlein pulse generators were resonantly pulse charged in the range of 3-75 kV and repetition rates of 1-1000 Hz. Both the voltages launched on the individual lines and the voltage pulse appearing across the series stack at the load were measured with a tapped water resistor connected to a Tektronix 7912AD transit digitizer. The full capacitance of the system was charged in about 120  $\mu$ s. A comparison of the measured charging voltages of each line and the voltage across the series stack yielded voltage gain information for the stacked Blumlein pulsed.

The UTD Blumlein pulsed commuted by thyatron or spark gaps have progressed from relatively simple, single-line devices to the most recent, compact stacked systems. Extensive characterizations of performance have demonstrated the versatility of these pulsed. It is shown that they can be developed into light and compact devices without degradation in their performance [1-5]. Voltage gains available from the stacked Blumleins now approach the number of lines.

## **2. Photoconductively-Switched Stacked Blumlein Pulsers**

Our recent efforts have resulted in demonstration of several intense photoconductively-switched stacked Blumlein pulsed. Presently, these devices operate with a switched peak power in the range of 50-80 MW and activating laser pulse energies as low as 300 nJ [5,6]. Examinations of output waveforms have indicated pulse durations in the range of 1-5 ns and risetimes as fast as 200 ps. Examples of the output voltage generated by a 2-line stacked Blumlein prototype with Blumlein length of 11 and 17 cm together with the photograph of the

pulser are given in Fig. 2. This pulser was constructed by connecting the corresponding high voltage and ground plates for each of the Blumleins to the switch electrode assembly. Blumleins with an impedance of about  $100\ \Omega$  were extended to the proximity of the stacking location, 11 or 17 cm from the switch electrodes, where the center, high-voltage conductor was terminated. Then the lines angled toward each other along with the dielectric, where they were stacked.

The lines were joined in series for about 2.5 cm, and the top and bottom plates were connected to a  $200\ \Omega$  non-inductive resistive load as shown in the top and bottom photographs of Fig. 2. At the switch assembly, the pulse-forming line was screwed to the electrodes in a low-profile geometry as shown in the middle photograph of Fig. 2. A semi-insulating liquid encapsulated Czochralski (LEC) type GaAs PCSS was used to commutate the pulser. The switch assembly was enclosed in a  $\text{SF}_6$  pressurized chamber. Pulse durations of voltage waveforms generated were proportional to the Blumlein lengths corresponding approximately to the two-way transit time of Blumleins. Peak voltage values for pulses presented in Fig. 2 were 98 kV, and corresponded to a voltage gain of 1.96.

A 4-line pulser was designed and constructed by combining two units of 2-line device with Blumlein lengths of 11 cm described above. A photograph of this pulser is shown in Fig. 3. The commutation assembly was reconfigured to contain two sets of electrodes. The pulse forming lines in each 2-line unit were bent in a manner to bring the stacking sections to the same location one above the other. The units were joined in series and the top and bottom plates were connected to a resistive load built from a stack of four  $100\ \Omega$ , non-inductive carbon disc resistors. This pulser is synchronously commutated by two GaAs PCSS and is capable of producing 1.5 ns output pulses with risetimes in the range of 200-300 ps. Table 1 present the best simultaneous and individual results obtained, to date, by switching the stacked Blumlein pulsers with high gain GaAs PCSS.



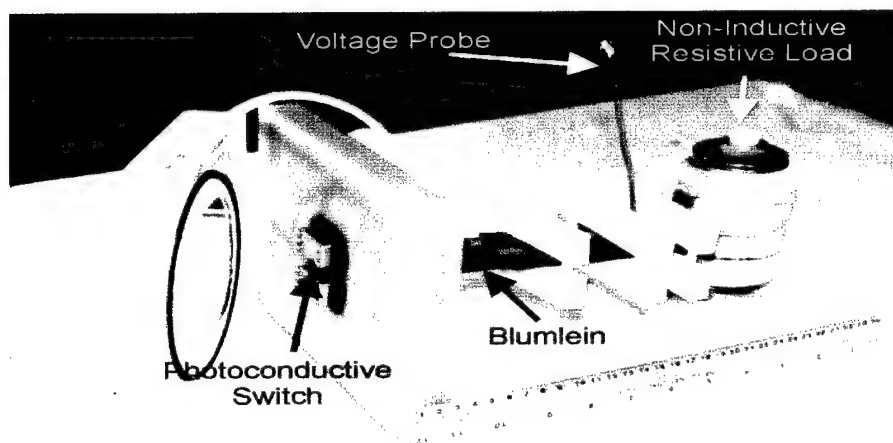
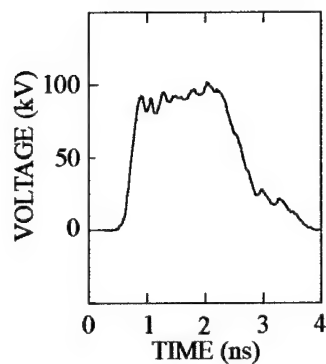
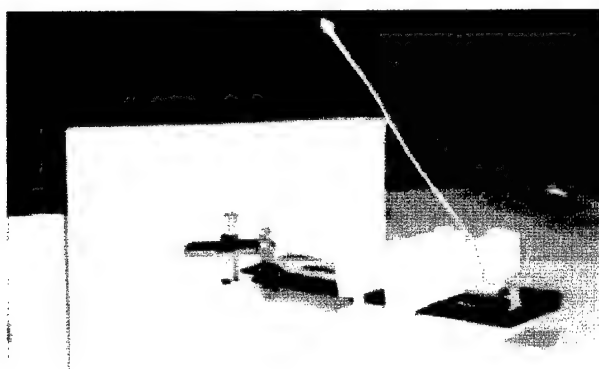
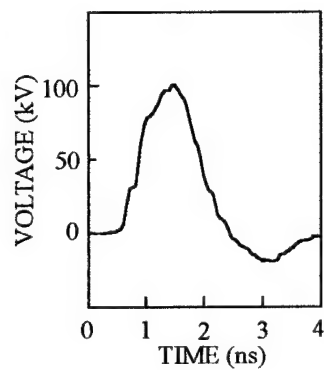
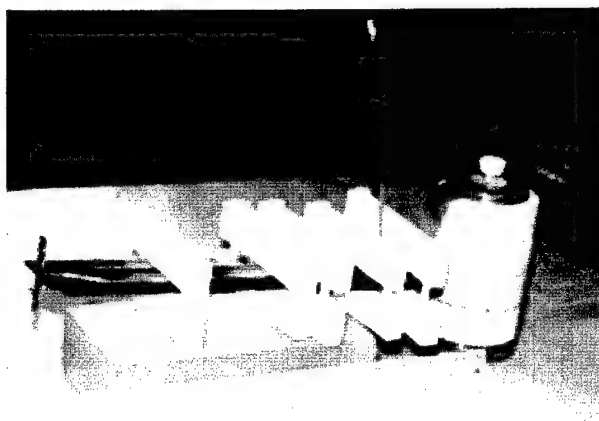


**Figure 2.** Output voltage pulses generated by the 2-line stacked Blumlein prototype shown at the bottom of this figure with pulse-forming lengths of 11 and 17 cm. Device was operated with a charging voltage of 50 kV. Top photograph shows the pulse-forming assembly connected to a resistive load. The middle photograph shows the pulse-forming section is being attached to the switch assembly.

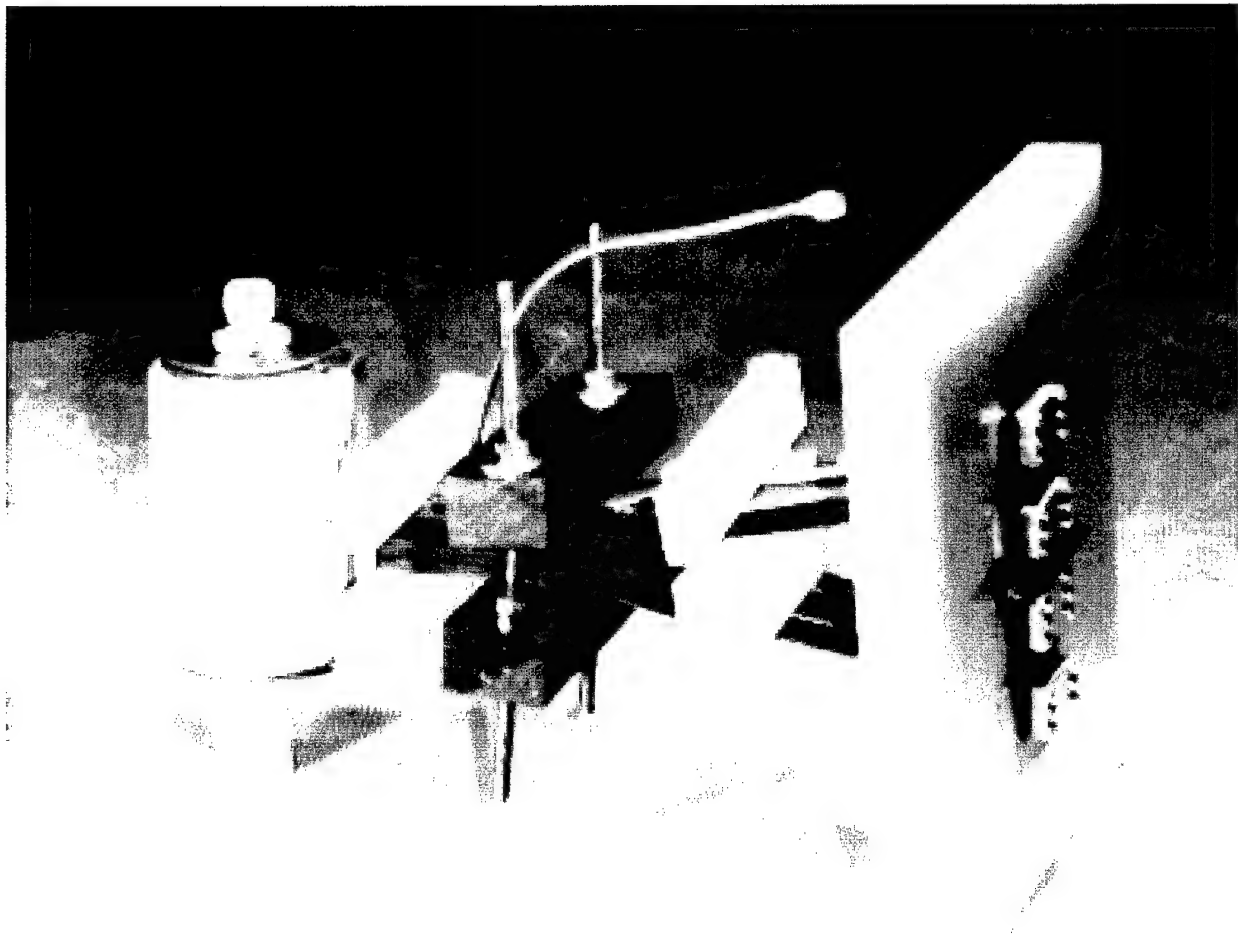


**Figure 3.** Photograph showing a 4-line pulser commutated by two photoconductive switches.

**Table 1.** Best simultaneous and individual test results obtained by commutation of 2-line stacked Blumlein pulsers with the high gain GaAs switches.

Parameters	Simultaneous Results		Individual Results
Switch Voltage	60 kV	30 kV	100 kV
Switch Current	1.2 kA	0.6 kA	2 kA
Pulse Risetime	200 ps	200 ps	150 ps
R-M-S Jitter	500 ps	500 ps	200 ps
Optical Trigger Energy	300 nJ	300 nJ	300 nJ
Repetition Rate	10 Hz	20 Hz	200 Hz
Electric Field	60 kV/cm	60 kV/cm	100 kV/cm
Stack Voltage	112 kV	57 kV	175 kV
Switch Lifetime	$1 \times 10^4$ pulses	$3 \times 10^5$ pulses	$1 \times 10^6$ pulses

### **3. High Gain Photoconductive Switch and Current Filamentation**

During the avalanche-mode switching of a pulser, the current is concentrated in filaments that extend from the cathode to the anode across the insulating region of the GaAs switch in a lateral configuration [13]. Carrier recombination results in the emission of characteristic band gap photons in the near infrared region that can be seen by an infrared viewer. We have observed these effects in experiments where laser diodes provided trigger photons for the avalanche commutation of the stacked Blumlein pulsers.

As soon as the avalanche is initiated, a single filament can be observed which approximately follows the collimated laser beam that was focused in two lines from the cathode to the anode. The top-right plots in Fig. 4 shows this behavior, which occurs the majority of time during switching. Multiple branches from the avalanche initiation point as shown in bottom-right plots in Fig. 4 were rarely observed prior to this work. Filamentary currents with densities of several MA/cm<sup>2</sup> and diameters of 15-300  $\mu$ m passing through a narrow channel can cause switch damage, especially at the contact points. Figure 5 shows a schematic presentation of the switch damage due to high current filaments. A greater number of filaments during each cycle of commutation reduce the stress on the switch, thereby increasing its lifetime.

Our efforts during this AFOSR grant have been directed to study and implement the broadening of the current channels in the avalanche photoconductive switch in order to improve lifetime and increase switching peak power. Our main efforts directed to study and use of amorphous diamond coatings at the switch electrode to enhance operation and lifetime of a PCSS in stacked Blumlein pulse generators.

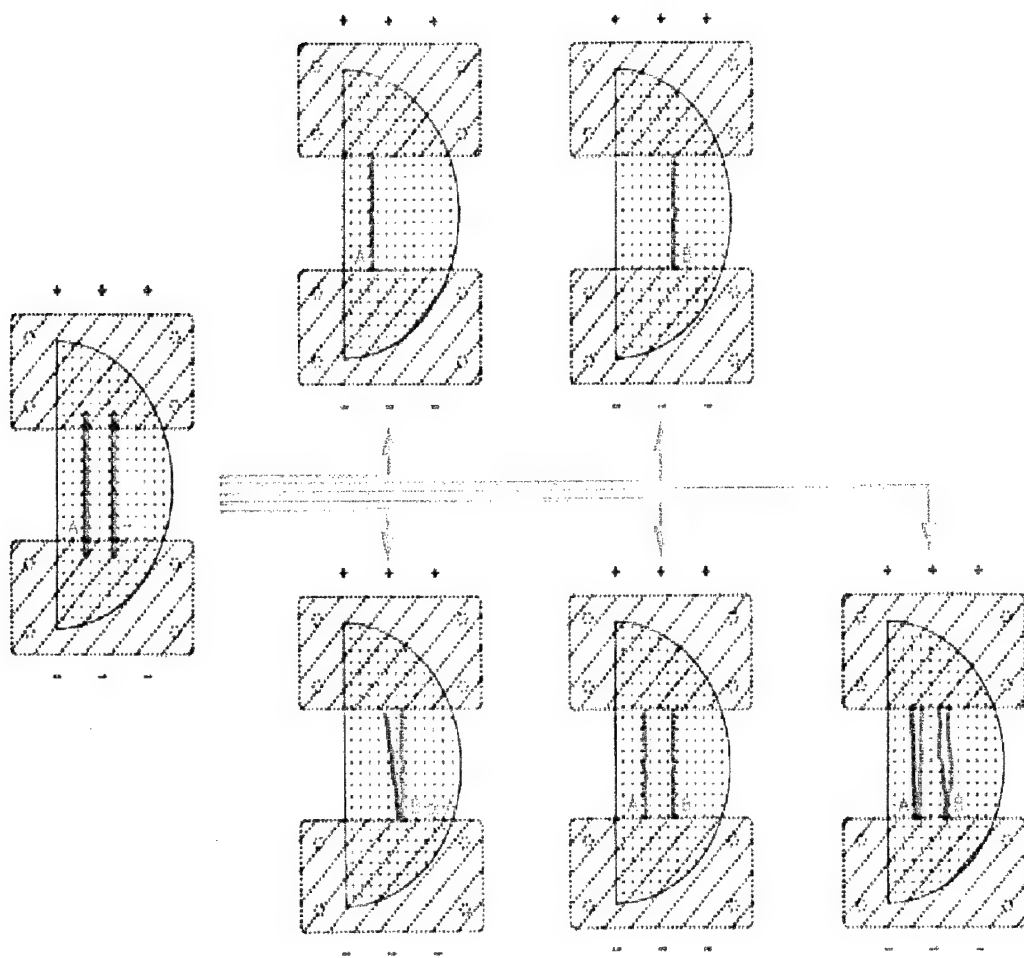


**Figure 4.** Schematic diagrams of a laser diode beam focused on the switch in two lines, and current filamentation seen with an infrared viewer.

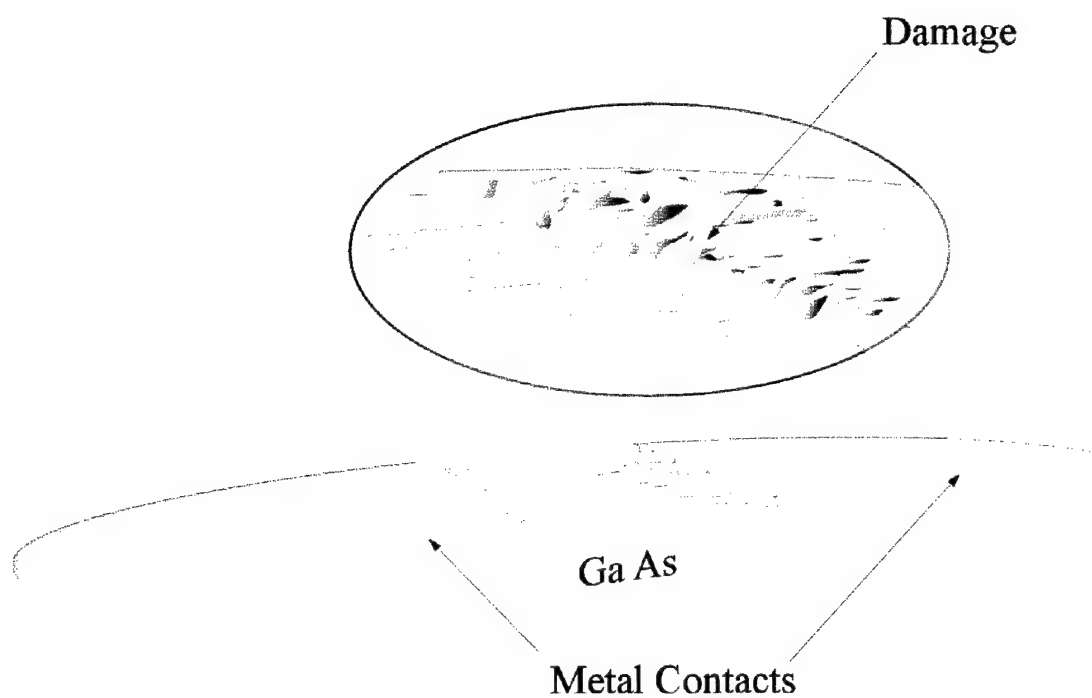


**Figure 5.** Schematic presentation of a GaAs high gain photoconductive switch with conventional metal contacts. Damage due to high current filaments is shown in the switch gap and metal electrode contact areas.

## AMORPHIC DIAMOND TREATMENT OF PHOTOCONDUCTIVE SWITCHES

### 1. Amorphic Diamond Deposition and General Properties

Amorphic diamond films have been produced by accelerating and quenching an intense laser plasma of  $C^{3+}$  and  $C^{4+}$  onto a cold substrate [14-16]. The diamond characteristics of this material have been evaluated by several analytical methods. Measurements agree in supporting  $sp^3$  contents of higher than 75% [15,16]. The films can be deposited on almost any substrate that is compatible with the vacuum without use of catalysts. Amorphic diamond seems to be a unique product of energetic condensation from  $C^{3+}$  and  $C^{4+}$  ions produced in a laser plasma. The original samples of this material were called amorphous ceramic diamond, an appellation shortened to "amorphic diamond" for convenience [14-16].

The importance of this nanophase diamond material has been suggested by reports of its unique mechanical properties [16-20]. It has been demonstrated that a favorable combination of low internal stress, hardness, elasticity and high bonding strength produce coatings with exceptional resistance to wear and erosion. Only 1-3  $\mu m$  coating of amorphic diamond could protect fragile substrates such as GaAs against erosive environments [18-20].

The deposition of Amorphic diamond by a laser plasma discharge has been realized with a Q-switched Nd:YAG laser at UTD. As described previously, the laser delivers 250-1400 mJ/pulse to a graphite feedstock in a UHV system at a repetition rate of 10 Hz [14-20]. For the production of nominal amorphic diamond films, the beam is focused to a diameter chosen to maintain the intensity on the target near  $5 \times 10^{11} \text{ W cm}^{-2}$  and the graphite is moved so that each ablation occurs from a new surface. A high current discharge confined to the path of the laser-ignited plasma is used to heat and process the ion flux further. Discharge current densities

typically reach  $10^5 - 10^6 \text{ A cm}^{-2}$  through the area of the laser focus, but the laser power alone is sufficient to insure that the resulting plasma is fully ionized.

A planetary drive system for rotating the substrates within the core of the plasma where they are exposed only to ions insures the simultaneous deposition of uniform layers of amorphous diamond over several substrate disks [14-19]. Figure 6 shows a schematic representation of the deposition system. Nominal coatings with 75%  $\text{sp}^3$  contents are produced with substrate holders 30-50 mm in diameter rotated in the core of the plasma at  $\alpha = 80^\circ$ , where  $\alpha$  is the deposition angle as shown schematically in Fig. 6. Despite the relatively high ion fluxes, bulk temperatures of the substrates monitored by a thermocouple do not exceed  $35^\circ\text{C}$  over deposition periods of several hours.

The impact of the laser plasma upon a substrate is equivalent to an irradiation with a very high fluence ion beam. Quenching of such energetic ions yields diamond while the condensation of neutral carbon produces only graphite [15,18]. Comparative micro-structural studies of films condensed from ions passing through the core and periphery of laser plasma have been performed extensively by scanning tunneling microscopy (STM). Different types of laser plasma diamonds have been identified and their diamond properties have been found to depend upon the energies of the ions condensed from the laser plasma [15,18]. The unique nodular structure of amorphous diamond films deposited by a core of laser plasma has been also reported [18,22] from examinations of films with STM. Typically, the nodule size ranges from 10 to 50 nm in diameter and imparts the properties of diamond found in the finished films [18]. A typical appearance of an amorphous diamond obtained by the transmission electron microscopy (TEM) is reproduced in Fig. 6.



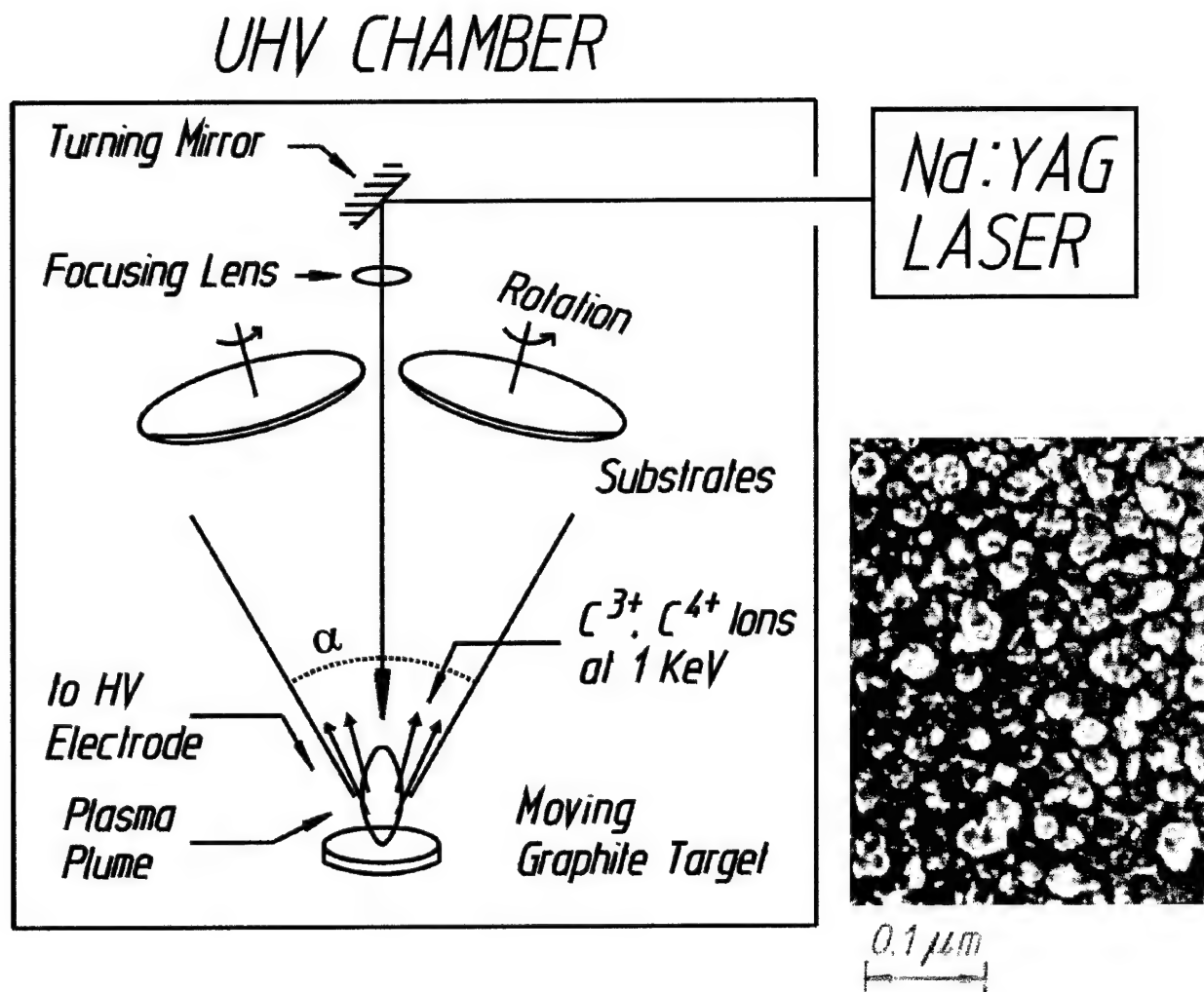


Figure 6. Schematic representation of the laser plasma discharge source used in this work to prepare amorphous diamond coatings. Diamond nodules are also seen in an image produced by TEM of a gold-coated replica of a film of amorphous diamond.

The diamond character has been verified by the agreement of structural morphology, density, optical properties,  $K_{\alpha}$  line energies and hardness. Nuclear reaction analysis (NRA) has proven the hydrogen content to be less than 0.5%. The nodules seem to be disordered mixtures of the cubic and the rare hexagonal polytypes of diamond that have no extensive crystalline planes along which to fracture. Since it is condensed from laser plasmas produced under conditions that are also optimal for the growth of interfacial layers, the films of amorphous diamond are strongly bonded to the substrates onto which they are condensed [19-21].

## **2. Heterojunction Devices Formed by Amorphous Diamond Coatings**

The application of diamond and diamondlike carbon (DLC) films to electronic devices are of considerable interest and the advantage of heterojunction devices formed by combining a wide band-gap coating with a narrow band gap substrate is clear. Depending on the preparation condition, coating behavior may widely vary between a semiconductor and an insulator [23-27]. Many diamond and DLC based heterojunction devices have been reported. However, control of the resistance of such coatings is necessary to produce an attractive semiconducting material for use with Si or GaAs in electronic devices [24-27]. In addition, diamond films transparent to visible wavelengths are limited in applications as a photoconductor or a field emitter because of their large band gap and high insulation characteristics [27]. Photosensitization by thin overcoatings and doping are required to overcome these limitations.

Amorphous diamond films with nodules of diamond in a matrix of more conductive phases of carbon might offer a viable alternative [14-22]. Recent field emission measurements have demonstrated that amorphous diamond emits electrons at high current densities when immersed in

modest electric field strengths and the electron emission could be adjusted by modifying the process parameters for the film production [28]. Furthermore, the emissivity of amorphous diamond films depends critically upon the packing densities of the diamond nodules and the amount of conductive phases in which they are embedded. Presently, electrical resistivity of amorphous diamond can be controlled in the range of  $10^2$ – $10^6$   $\Omega$  cm by adjusting the deposition parameters.

Deposition of thin films of amorphous diamond on Si and GaAs has produced rectifying heterojunctions with highly asymmetric I-V characteristics and a reverse breakdown strength greater than  $10^9$  V/m [28-31]. Amorphous diamond coatings were deposited on one side of Si substrates and electrodes were attached to either side using conducting silver paint and epoxy. The grid like conducting electrodes was painted on the coating sides. For these measurements a Keithley 237 high voltage source-measure unit was used to provide constant voltage bias while monitoring the current through the sample. To avoid heating the sample the measurements were carried out with pulsed voltage sweep having on and off times of 50 and 450 ms, respectively. For measurements of forward diode characteristics, diamond coating was biased negative with respect to the substrate. Under white light conditions, the total luminous flux received on a unit area (illuminance) of the sample was measured by a light meter. Typical I-V characteristics measured for a 0.23  $\mu$ m nominal amorphous diamond on the p-type Si (100) with a resistivity in the range 20-60  $\Omega$  cm are shown in Fig. 7. The device was examined under the dark and white light conditions with bandpass optical filters.

The rectifying behavior seen in Fig. 7 was attributed to the amorphous diamond /Si junction. This was verified by placing silver epoxied electrodes on bare Si substrates and observing symmetrical and ohmic current-voltage behavior with change in voltage polarity.

Current increases of one to two orders of magnitude were observed when the device was exposed to light. Under forward biased conditions there were only slight current increases for the light exposure.

During this AFOSR Program, the spectral response was estimated with bandpass optical filters over the wavelength range 350 – 1100 nm. One example is shown in Fig. 7. For all devices fabricated the maximum of the photoresponse was found to be in the range 600 – 900 nm. This is consistent with the earlier measurements indicating an optical gap for the laser produced amorphous diamond films lying between 1 – 2.2 eV [14-20].

The relative spectral response for a device comprised of a 0.23  $\mu\text{m}$  nominal [5] amorphous diamond on the p-type Si (100) with a resistivity in the range 20-60  $\Omega\text{ cm}$  is shown in Fig. 8. The plot obtained with the device operated under the reverse bias at 50 V. The optical gap measured for the nominal amorphous diamond was 1.45 eV, consistent with the spectral response seen in Fig. 8.

Current-voltage properties have been also studied for the amorphous diamond on n-type silicon. It was found that rectification was in the same direction with diamond layer acting as the cathode. Figure 9 compares the I-V characteristics, in the reverse biased conditions, for the nominal amorphous diamond coatings 0.23 and 0.13  $\mu\text{m}$ -thick on the n-type and p-type Si substrates, respectively. The measured reverse breakdown voltage in excess of 425 V for a 0.13  $\mu\text{m}$ -thick coating on p-type Si gives an electrical breakdown strength greater than  $3 \times 10^9\text{ V/m}$  if the entire diamond film is assumed to be depleted. The high electrical breakdown strength for amorphous diamond suggests that carrier velocity saturation in high field strength is allowed and the electron-electron scattering is of the same order as that in crystalline diamond [22].

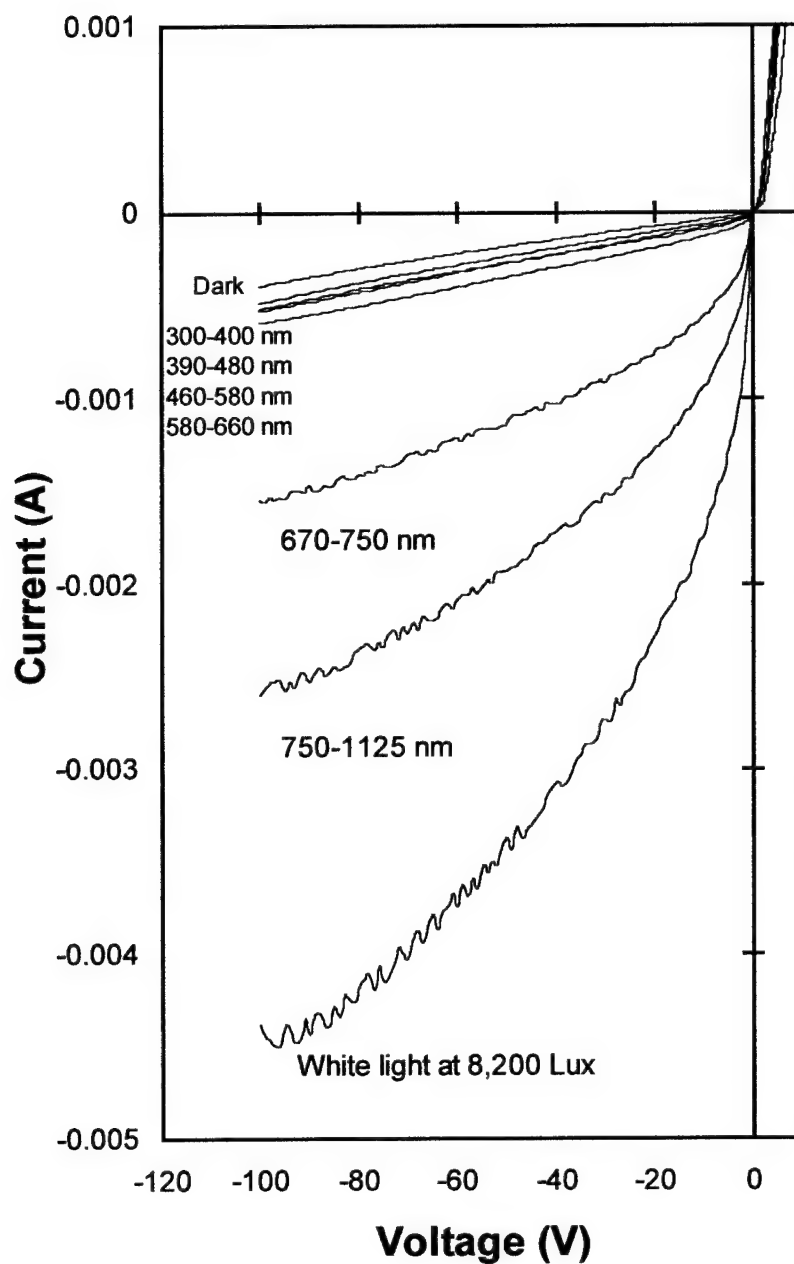


**Figure 7.** Current –Voltage characteristics measured for a nominal amorphous diamond deposited on a p-type Si in the dark and under white light conditions with bandpass optical filters.

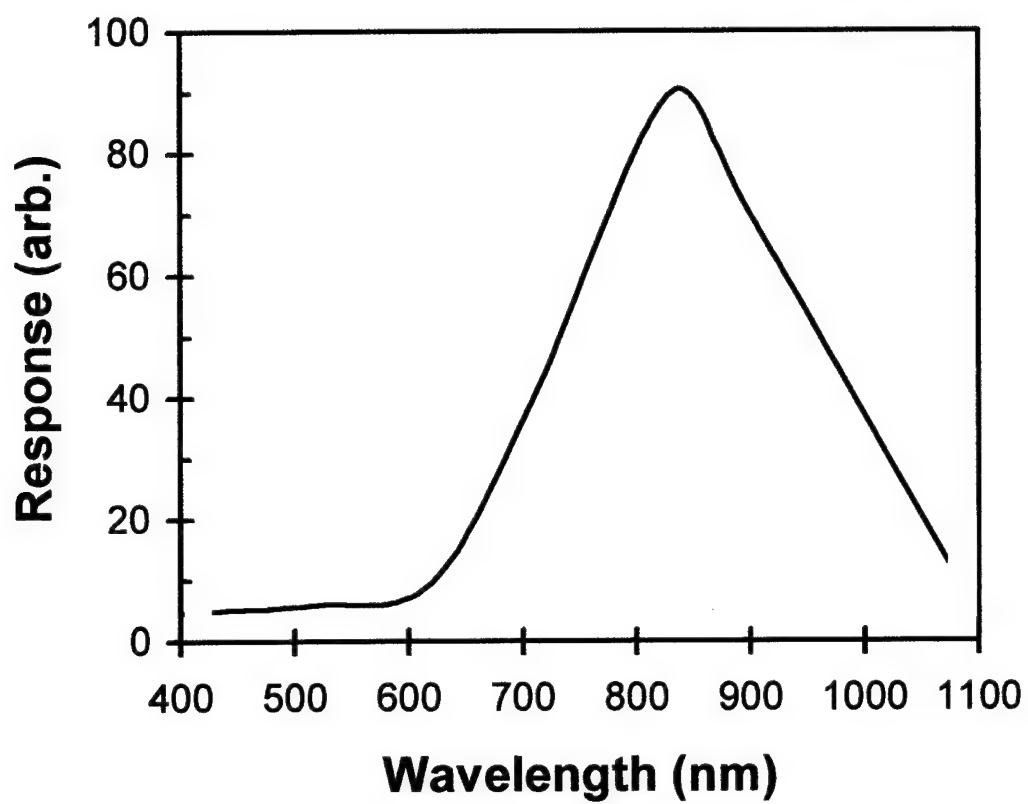


**Figure 8.** Spectral response for an amorphous diamond/ Si heterojunction operated under the reverse bias at 50 V.

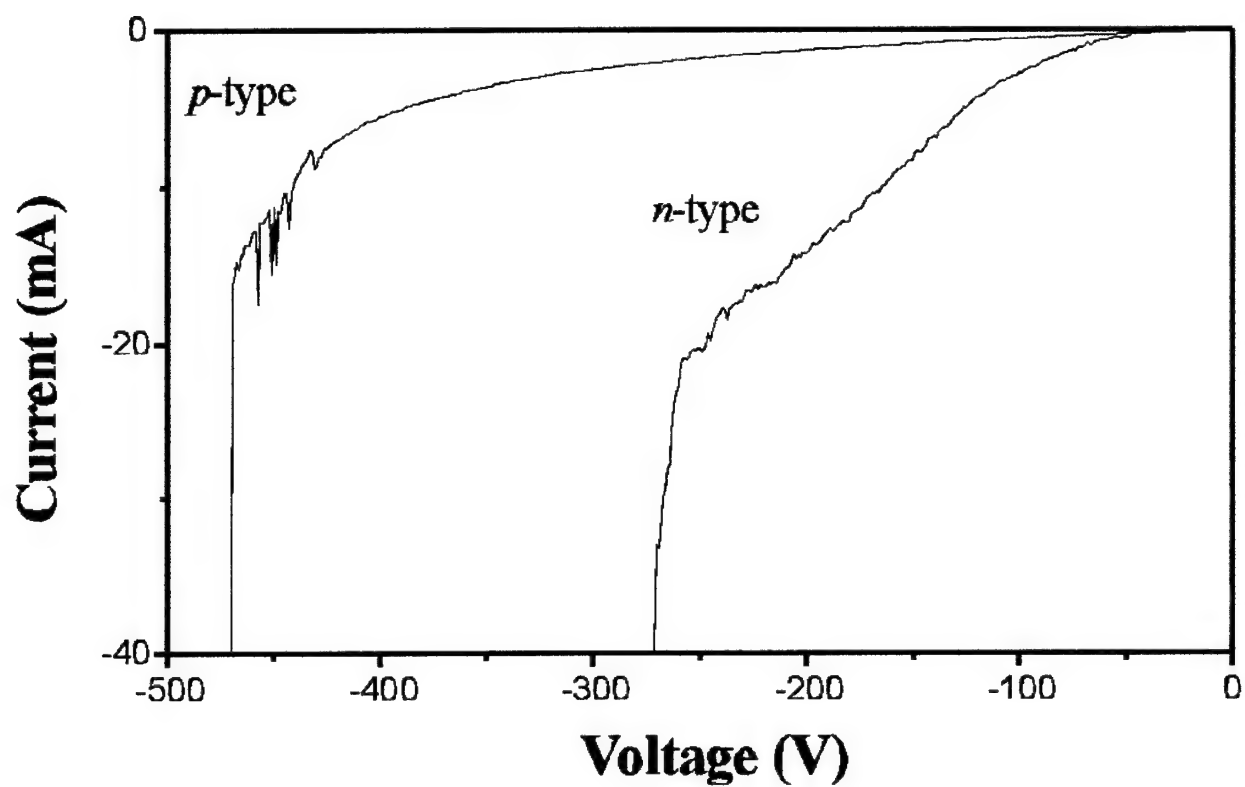


**Figure 9.** Current-Voltage characteristics showing the breakdown voltages for the nominal amorphous diamond films on p- and n-type Si substrates. Measurements performed in the dark under reverse bias conditions.

In almost all junctions fabricated, the reverse breakdown voltage of the amorphous diamond on n-type Si appeared to be less than that on p-type Si. As shown in Fig. 9, a thicker film of amorphous diamond on n-type Si had a lower reverse breakdown voltage and the breakdown strength was about  $1.1 \times 10^9$  V/m. In addition, for the sample comprised of n-type Si, a soft breakdown of reverse voltage is seen at around 60 V. This may be due to the release of trapped negative charges when the amorphous diamond is slowly depleted at reverse bias voltages above 60 V.

We have performed experiments to test these amorphous diamond / silicon rectifying devices as low voltage photoconductive switches. For this purpose, a single Blumlein with line length of 3.6 m and Blumlein impedance of  $50 \Omega$  was constructed. Output of the Blumlein was connected to a  $50 \Omega$ , non-inductive carbon disc resistor. Switching and storage capacitance of the Blumlein was about 1 nF. An amorphous diamond /silicon device was connected to the Blumlein in a reversed biased configuration where the anode electrode was attached to amorphous diamond side. Figure 10 presents a photograph of the Blumlein switch assembly where the junction device is connected. A pulse charging power supply was used to charge the Blumlein in about 50  $\mu$ sec, after which a trigger pulse from a master oscillator Q-switched an Nd:YAG laser and provided trigger photons in a 40-ns FWHM pulse for the switch activation. These photons were delivered to the switch by means of a diverging lens, which allowed a few mJ/pulse over the surface area of diamond coating in the device. Output voltage waveform is reproduced from our earlier work in Fig. 10 for the charging voltage of 100 V. It is interesting to note that these rectifying devices acted as linear photoconductive switches where switch voltage follows closely the activating laser pulse.



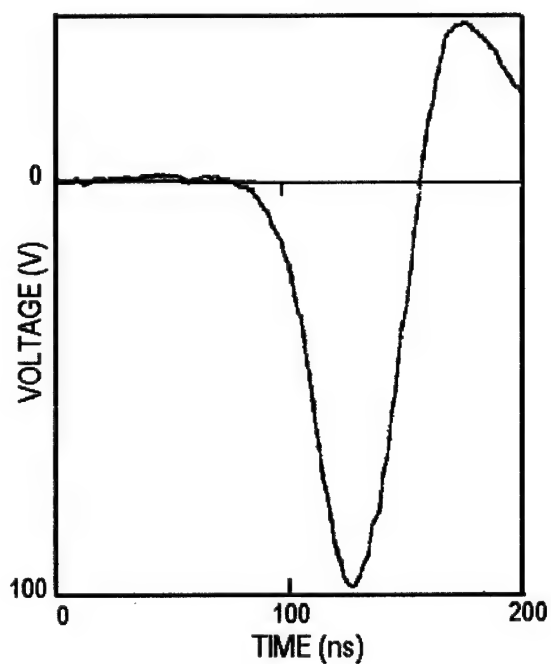
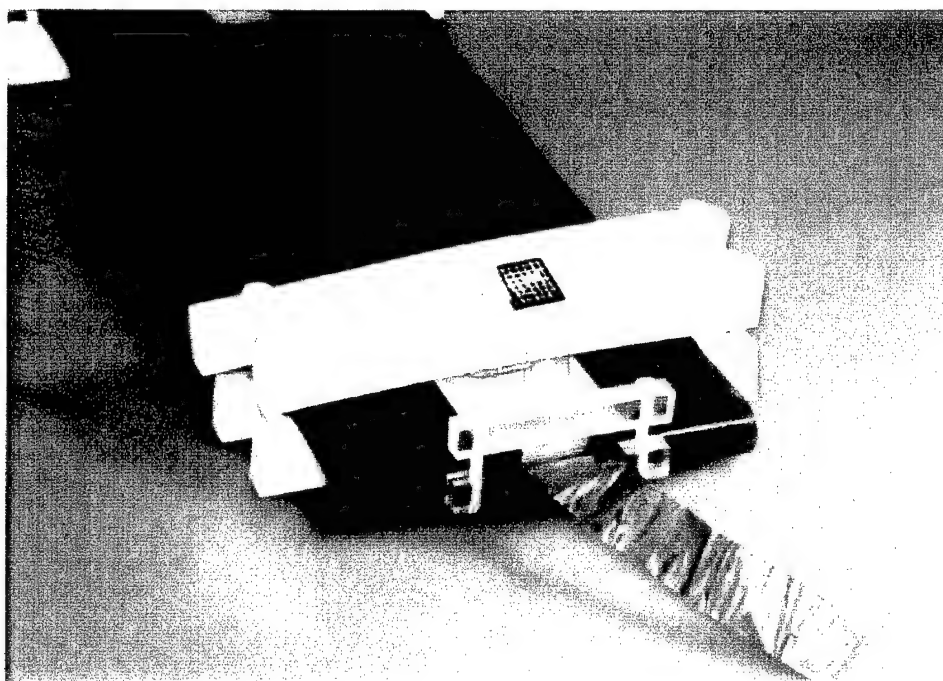


**Figure 10.** Photograph of the Blumlein switch assembly where the amorphous diamond/ Si device is connected. A voltage waveform generated by the pulser is shown here for reference. The charging voltage was 100 V.

### 3. Diamond-Coated Photoconductive Switch

During this AFOSR Program, amorphous diamond coatings were deposited on one side of semi-insulating LEC grown GaAs substrates with resistivity of about  $1.0 \times 10^7 \Omega \text{ cm}$ , the type used in our Blumlein pulsers as the photoconductive switch material. Electrode copper foils were attached to either side using conducting silver paint and epoxy as shown schematically in Fig. 11. Electrodes were attached to opposite sides of the switch, and conduction was through bulk of the GaAs, with the switch gap settings of 0.5, or 5, and/or 10 mm. A Keithley 237 high voltage source-measure unit was used to provide constant voltage bias in the range 0-600 V while monitoring the current through the sample. For measurements of forward diode characteristics, diamond coating was biased negative with respect to the substrate as shown in Fig. 11.

Typical current-voltage characteristics measured for 0.5- $\mu\text{m}$  and 1.0- $\mu\text{m}$  nominal amorphous diamond films on semi-insulating GaAs are shown in Fig. 12. An electrode gap setting of 0.5 mm was chosen for this measurement. For comparison, the I-V plot for an uncoated similar GaAs substrate is included in this figure. The rectifying behavior for the coated sample seen in Fig. 12 was attributed to the amorphous diamond/GaAs heterojunction because the I-V plot for the uncoated sample showed symmetrical and ohmic character with change in the voltage polarity. The I-V characteristics differ considerably for the diamond-sample, especially for the forward current region where the coating side was biased negative.

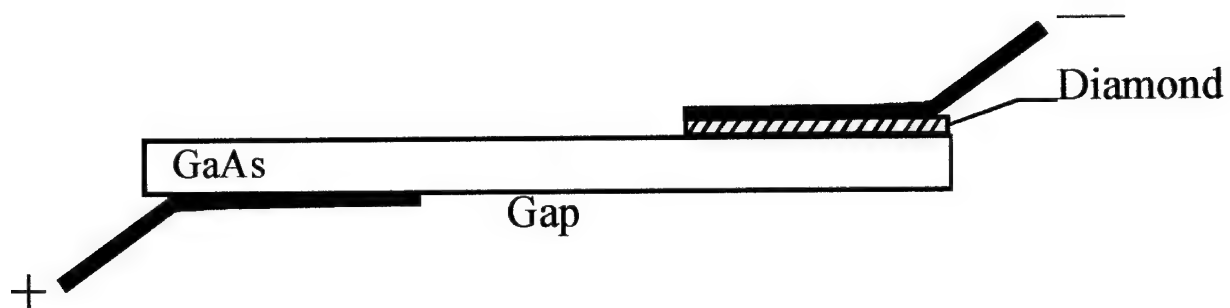


**Figure 11.** Schematic presentation of a switch sample cross section used for forward I-V measurements.

The rapid current increase in the forward direction for the coated sample has been attributed to tunneling of electrons from amorphous diamond to the conduction band of GaAs, a process similar to Fowler-Nordheim tunneling [28]. As seen in Fig. 12, the 1.0- $\mu\text{m}$  diamond coating enhances the current increase in the forward direction when compared to the sample with a 0.5- $\mu\text{m}$  coating. The rectifying character under reverse bias is clearly seen for both coated samples, with the thicker film reducing the process of rectification.

Current-voltage properties were also studied for the amorphous diamond coatings on a semi-insulating GaAs switch with a gap setting of 5 mm. Results are presented in Fig. 13 for an uncoated sample and for two samples of diamond-coated GaAs switch. Again, a symmetrical and ohmic current-voltage behavior is seen for the uncoated sample, and the I-V characteristics differ considerably for the coated samples, especially for the forward current region where the coating sides were biased negative. The rectifying character under reverse bias is enhanced for the sample coated with the thinner amorphous diamond film.

In this work, current-voltage measurements were also performed at higher bias voltages with switch samples coated with 1.0 and 2.0  $\mu\text{m}$  amorphous diamond coatings. Results are shown in Fig. 14 for the GaAs switches with a gap setting of 10 mm in the opposed configuration shown in Fig. 11. In agreement with results shown in Figs. 12 and 13, the sample with the thicker coating produced enhanced tunneling of electrons from diamond to the GaAs conduction band, while the thinner coating produced better rectification under reverse bias voltages.

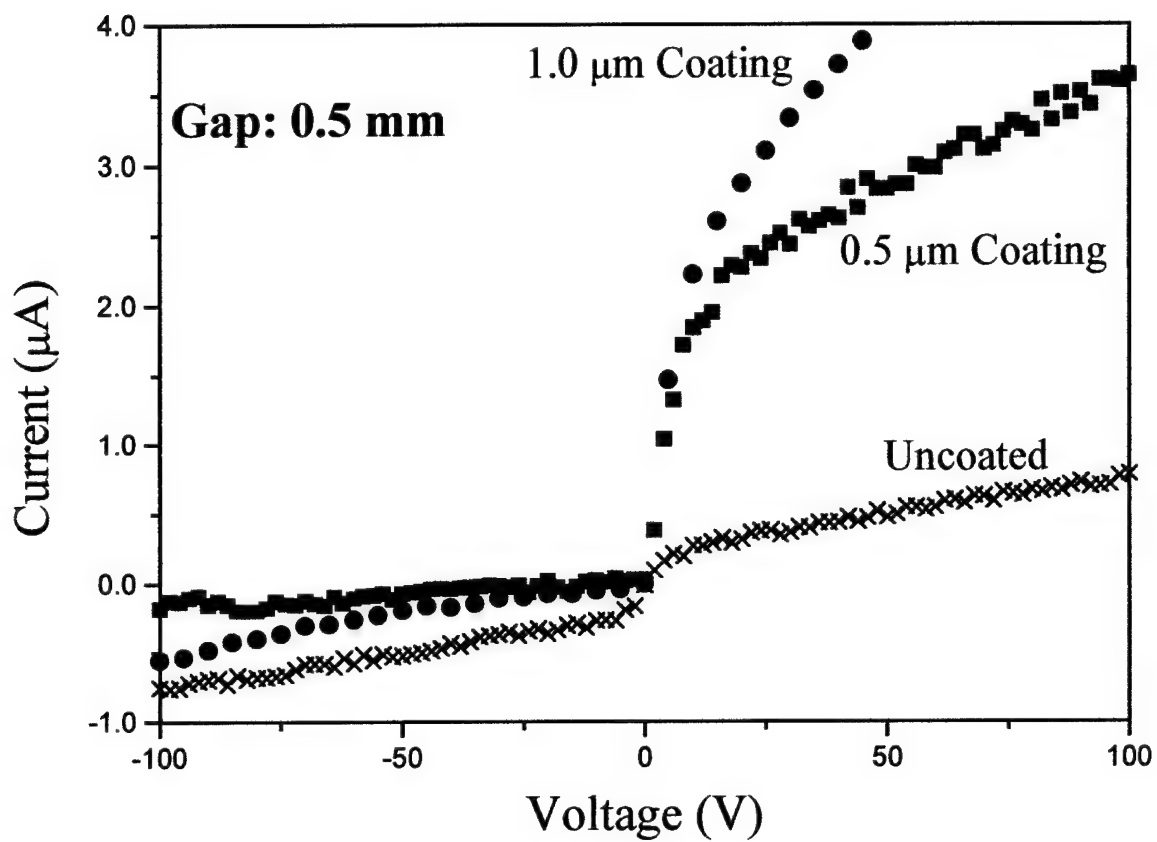


**Figure 12.** Current-voltage characteristics measured in the dark for an uncoated sample and two samples of a diamond-coated GaAs switch substrate with a gap setting of 0.5 mm.

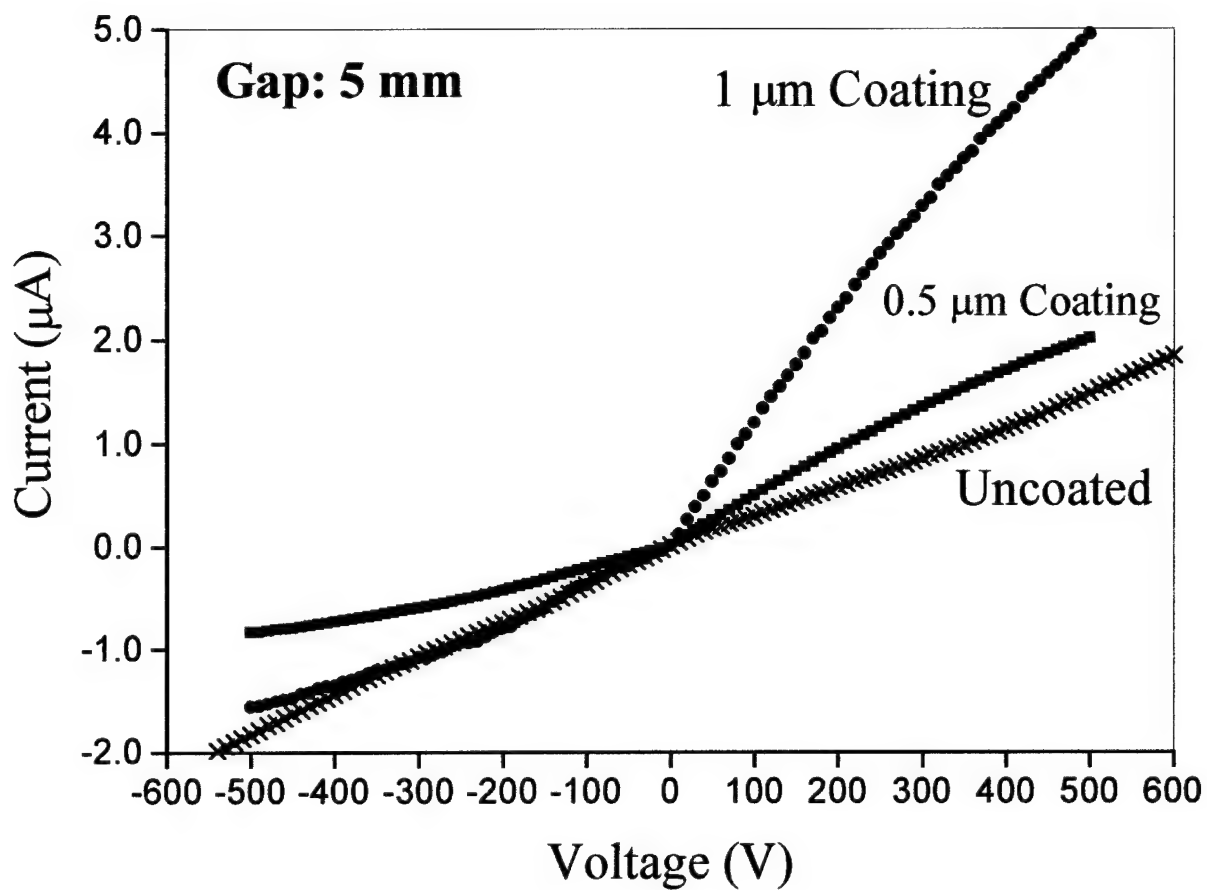


**Figure 13.** Current-voltage characteristics measured in the dark for an uncoated sample and two samples of diamond-coated GaAs switch substrate with a gap setting of 5 mm.

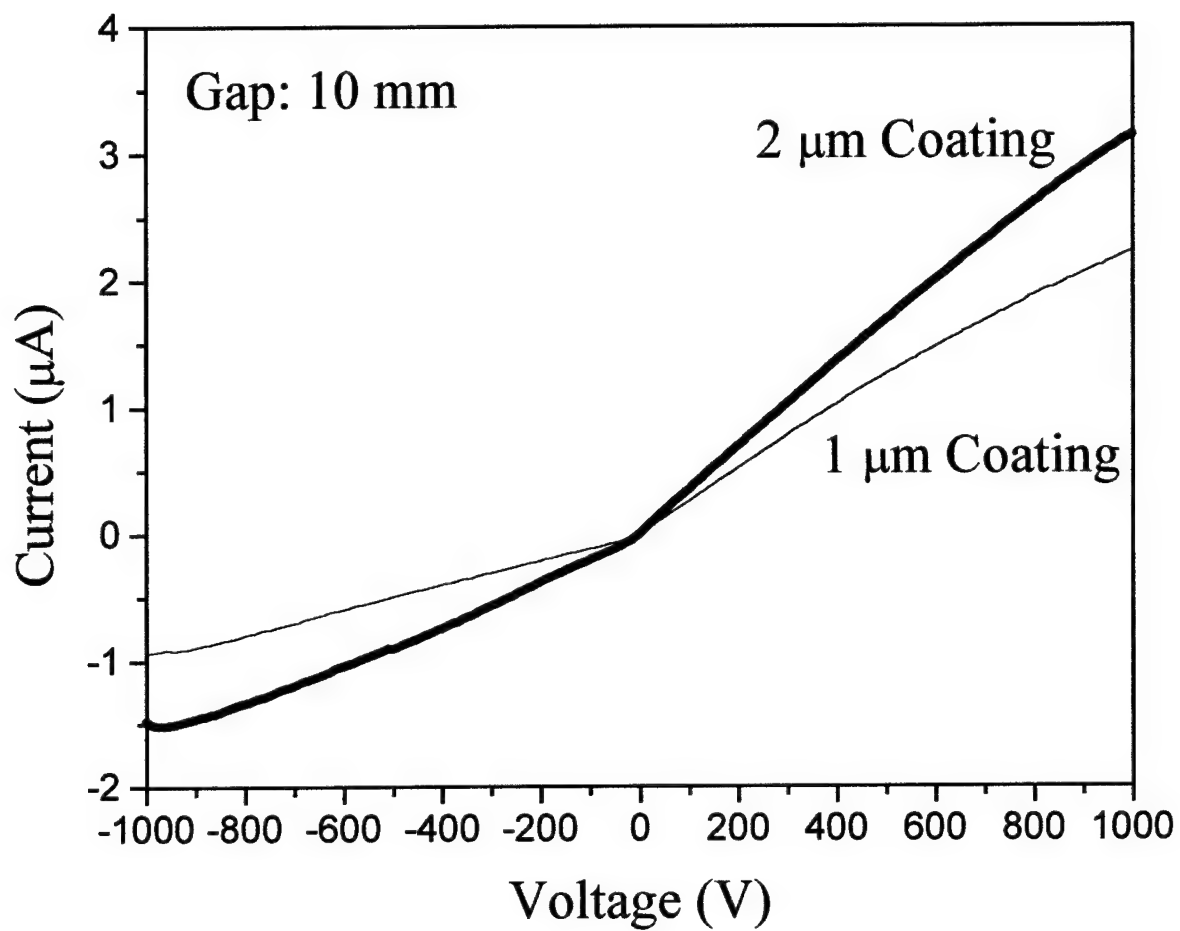


**Figure 14.** Current-voltage characteristics measured in the dark for two samples of diamond-coated GaAs switch substrates.

We also investigated the current injection afforded by the amorphous diamond at high DC voltages. For these studies we used a PTS 130 Hipot acquired from the High Voltage, Inc. It provided constant voltage while monitoring the current through the sample. Measurements obtained by biasing the diamond coating negative with respect to the substrate. Test samples were placed in a chamber filled with high pressure  $\text{SF}_6$  gas to avoid flash over during the experiment at high voltages. Current-voltage characteristics measured for a 0.5- $\mu\text{m}$  nominal amorphous diamond on the GaAs with a gap setting of 10 mm is shown in Fig. 15. For comparison, the I-V plot for an uncoated similar GaAs substrate with an electrode gap of 10 mm is also presented in this figure.

Of importance to our studies, is the rapid current increase in the forward direction as seen in Figs. 12-15. The tunneling of electrons from amorphous diamond to the conduction band of the GaAs provides pre-avalanche sites for the operation of diamond-coated PCSS, and thereby diffuses the conduction current.

#### **4. Junction Conduction Mechanism**

The amorphous diamond forms a heterojunction with Si and or GaAs crystalline substrates [29-31]. The two joined semiconductors have different characteristics. However, the Fermi level of the formed device still must equilibrate throughout. The movement of the position of the Fermi level within the band gap of a semiconductor is affected by the doping type and concentration in the semiconductor. Shifts in the relative positions of the conduction and valence bands of the two semiconductors raises or lowers the barriers to conduction for electrons or holes.



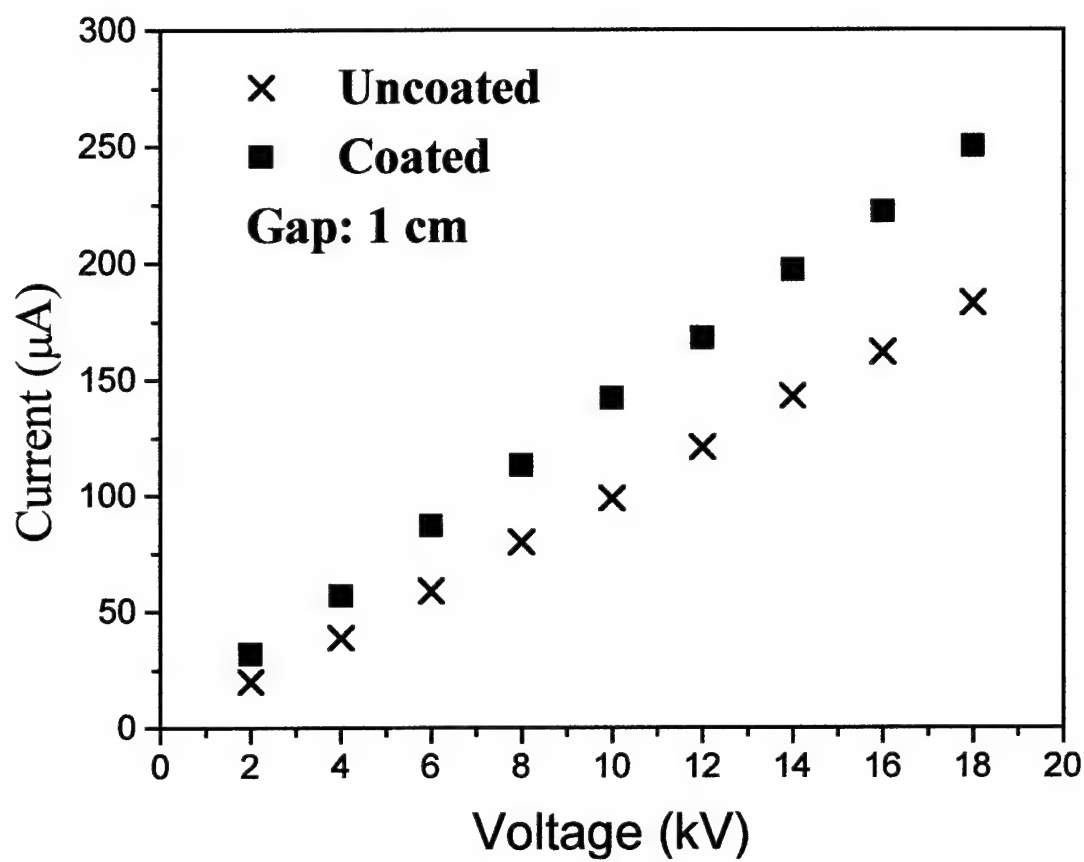


**Figure 15.** High voltage I-V characteristics measured in the dark for an uncoated sample and a sample of diamond-coated GaAs switch substrate with a gap setting of 10 mm.

An important assumption in this picture of a heterojunction is the existence of perfect transition, one without crystalline lattice defects, across the junction interface from one semiconductor type to another. Lattice defects create energy states that are not restricted from being in the band gap energy position. Defect energy sites are easily formed at the interface of heterojunctions possessing even a relatively small lattice constant mismatch.

An amorphous semiconductor, such as the amorphous diamond, which is replete with defect energy states, may possess an even greater surface density of defect states. The role played by such an amorphous semiconductor in interfacing another semiconductor would be similar to that played by a metal in a metal-semiconductor contact. The action of this junction with rectification in a single direction in spite of substrate doping, is consistent with the Fermi level at this interface being kept at a fixed energy level somewhere in the band gap of the semiconductor by the surface states of the substrate, independently of the Fermi level in the bulk [32].

The joining of an amorphous semiconductor to a single crystal semiconductor produces a junction that is expected to exhibit qualitatively different behavior since the predominant conduction mechanism on the amorphous side is hopping or thermally assisted tunneling near the Fermi level. Dohler and Brodsky [33] have presented a study of the behavior of such heterojunctions. They deduced that the density of states on the amorphous side is much larger than the doping concentration of the crystalline side. Their results show that the transport properties of such a junction bear resemblance to a metal semiconductor junction since the conduction of the amorphous side occurs near the Fermi level. Additionally, they argue that there is no image force potential present, hence, Schottky barrier lowering does not appear. They

also submit that interface states may influence the current generation recombination centers, and that they have a drastic effect on the potential profiles of the junction [33].

Donnelly and Milnes have extended studies for other types of heterojunctions. For example for the nGe/pGaAs heterojunctions, they concluded that the tunneling currents predominate across the entire junction. The evidence seems to indicate that interface states dominate the current flow mechanism owing to the inherently large density of states at the interface. Consequently, very little, if any, minority carrier injection current is observed [34]. The operation of the amorphous diamond/Si or GaAs heterojunctions could likely fit in with the general ideas of transport presented by Dohler and Brodsky, and Donnelly and Milnes.

It appears that interface states predominate at the junction of amorphous diamond and a crystalline semiconductor such that the barrier height and direction of rectification are independent of doping type and concentration in the substrate. The heterojunction exhibits Schottky barrier properties at least to the extent that the reverse bias I-V characteristics are bias voltage dependent. This is because the free charge density of the amorphous diamond is higher than that of the crystalline semiconductor and hopping conduction occurs at or near Fermi level similar to the conduction through a metal. The effect of image-force lowering of the Schottky barrier is very slight, possibly due to the small charge density of the amorphous diamond relative to that of metal. Carrier transport through the device is accomplished by a combination of tunneling through the amorphous diamond to the interface whereupon recombination occurs with the emission current coming from the crystalline semiconductor side where the interface states act as recombination centers. The process is similar to Fowler-Nordheim tunneling. Further studies are required to obtain the precise mechanism of heterojunction operation.

## 5. Switch Behavior with Diamond Coating

During efforts for this Program, we have studied the current-voltage characteristics for the diamond coated and uncoated GaAs switch materials with the three different gap settings. As described earlier, the measurements for uncoated samples show a symmetrical and ohmic behavior with change in voltage polarity for all gap settings examined in this work. The dynamic resistance values obtained from the slopes of these plots are consistent with the resistivity of semi-insulating LEC grown GaAs substrates used in this work, about  $100 \text{ M}\Omega \text{ cm}$ . As expected the dynamic resistance for the uncoated switch with a 10-mm gap setting is about twice and 21 times of the samples with the 5-mm and 0.5-mm gap settings, respectively.

Figure 16 shows the current-voltage plots for three switches with the different gap settings each coated with a strip of  $1\text{-}\mu\text{m}$  amorphous diamond. Forward characteristics correspond to measurements performed with the switch cathode coated with diamond as schematically shown in Fig. 11. The reverse characteristics provide the response for the switch with the anode side coated with amorphous diamond.

The rectifying character under reverse bias seen in Figs. 12-14 may be used to reduce switch leakage current. Examination of I-V plots in Fig. 16 shows the forward and reverse bias dynamic resistance values are increased and decreased, respectively, as the corresponding switch gap settings is reduced. The trend seen in Fig. 16 is a complex combination of the junction character and the dynamic resistance of bulk GaAs in each switch, especially for the reverse bias voltages.

Examination of the forward I-V characteristics indicates that the dynamic resistance of the bulk GaAs is the dominant factor for the coated sample behavior. For Example the forward

conduction current for the sample with a 0.5 mm gap at a particular voltage  $V$  is about the same as conduction currents for the samples with 5 and 10 mm gaps at bias voltages 11V and 22V, respectively. However, for the reverse bias condition the I-V behavior is probably affected by combination of comparable dynamic resistances for the junction and bulk GaAs with a complex de-convolution factor.

The diamond/GaAs heterojunction response is limited to a very thin layer across the cross section between amorphous diamond and GaAs that includes coating thickness. This implies that while the charging voltage applied to the photoconductive switch electrodes during the off-state phase are usually in the range 10-100 kV [5,28], the actual voltage driving the heterojunction behavior could be as little as only a few volts.

The effect of diamond coating on off-state switch conduction is a combination of the heterojunction behavior and the bare GaAs performance under bias voltages applied. Thus, the I-V behavior of the diamond coated switch with the 5 mm gap setting should be equivalent to that of the coated switch with the 0.5 mm gap combined in series with an uncoated switch with a 5-mm gap.

Similarly, the characteristic of diamond-treated switch with the 10-mm gap is equivalent to the coated switch with 0.5-mm gap plus an uncoated switch with a 10-mm gap. Furthermore, the coated switch with the 10-mm gap is equivalent to the coated switch with the 5-mm gap plus an uncoated switch with a 5-mm gap. These assertions were found to be accurate by study and examinations of I-V plots such as those shown in Figs. 12 and 13.

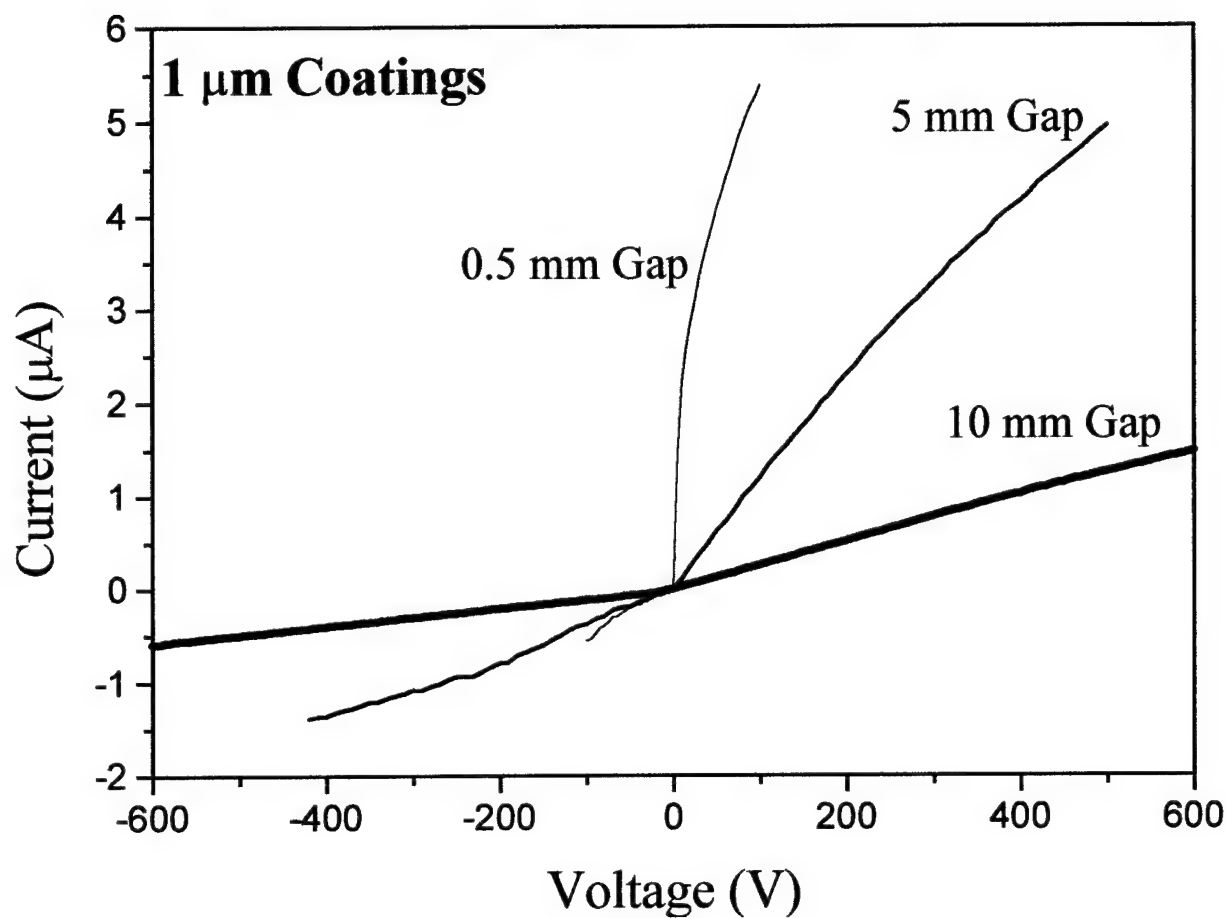


**Figure 16.** Current-voltage characteristics measured in the dark for three samples of diamond coated GaAs switch substrates with gap settings of 0.5, 5 and 10 mm.

## SWITCH LIFETIME STUDIES

The switch/electrode configuration used in the PCSS lifetime studies is a part of a low profile switch assembly [5,28] that facilitates the use of a single photoconductive switch in the pulser, as can be seen in Fig. 17. The electrode assembly allows for operation of PCSS in either lateral or opposed configurations. Layers of Kapton insulator are placed between the switch and the base electrode to restrict the current path through the top electrode holders in the lateral configuration. In the opposed configuration, switch is placed to contact one of the base electrodes on one side and the other top electrode holder on the other side. Layers of Kapton are used to isolate the switch from the base electrode on one side and the top electrode holder on the other side. The current path is through one of the top electrode holders into the GaAs bulk and through the other base electrode. In experiments with both switch/electrode configurations, top copper electrode holders are connected to the base electrodes by means of several screws as shown in Fig. 17.

For the lifetime studies, the pulse forming lines from a prototype stacked Blumlein pulser were connected to the bottom of base copper electrodes, which were cast in a G-10 plastic plate. Each switch was fabricated from one half of a semi-insulating LEC grown GaAs wafer with a diameter and thickness of 5 cm and 0.5 mm, respectively. It was held in place by means of two copper holders screwed to the electrodes. Commutation of the switch was triggered at 905 nm by focusing the LD-220 laser diode array beam in two straight lines across the switch gap from cathode to anode.

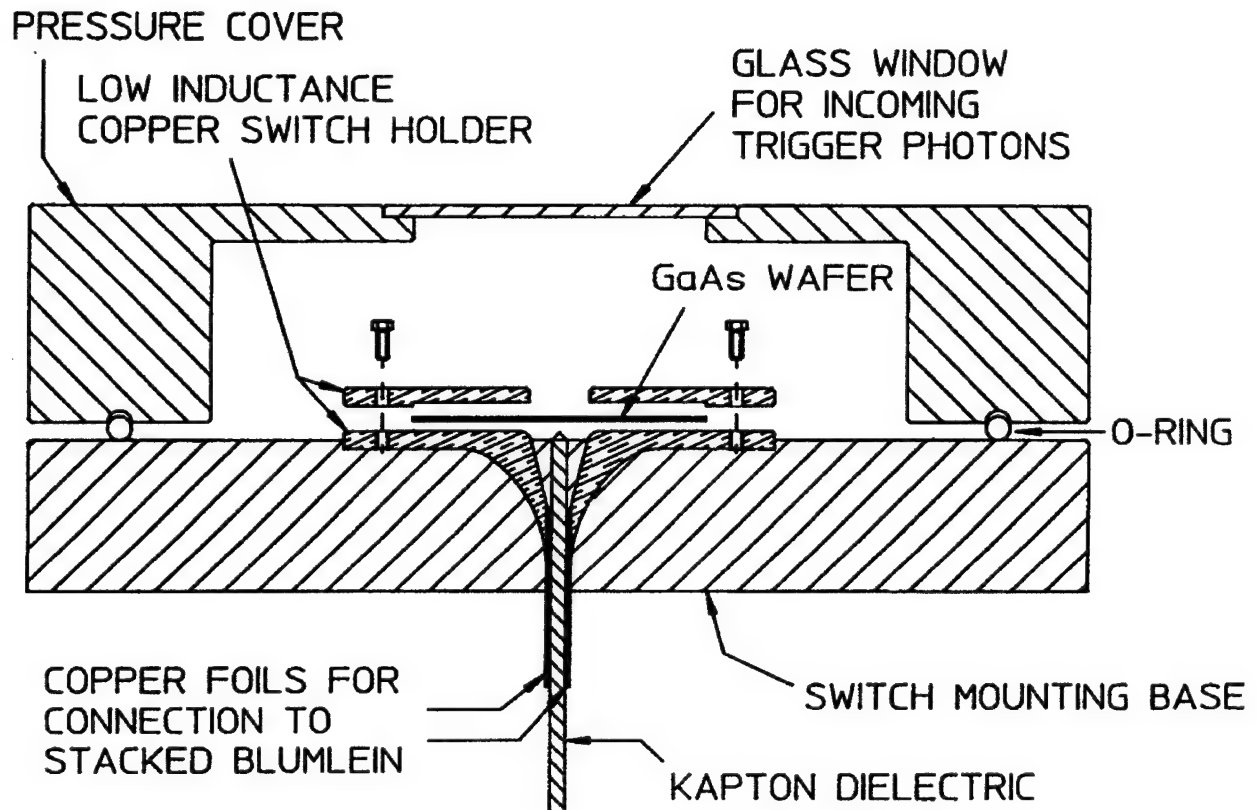


**Figure 17.** Schematic drawing of the cross section of the switch assembly used in this work for switch longevity tests.



Improvements in the PCSS switch operation and lifetime have been examined in a lateral configuration by coating the triggered face of GaAs switch cathodes with strips of highly adhesive films of amorphous diamond. With the application of amorphous diamond, not only the switch lifetime was increased, but also the damage at the cathode contact was found to be less than that found for the anode contact [28]. This indicated that the diamond coating protected and hardened the cathode side.

During this work, we studied the lifetime of three GaAs switches with a 1-cm strip of 0.5- $\mu\text{m}$  diamond coatings deposited on the switch at electrode locations: cathode, or anode, and/or both cathode and anode. All switches were installed in an opposed configuration similar to that shown in Fig. 11. A switch gap of 5 mm was chosen for this study. The switch was tested at 18 MW (0.6 kA and 30 kV) until they failed. Under similar conditions of experiments and switch configuration, we performed a switch longevity experiment with an uncoated GaAs switch. Results of these studies are given in Table 2. Test results indicate significant switch lifetime improvement by the application of amorphous diamond.

**Table 2.** Results of switch longevity tests.

<b>Test Condition</b>	<b>Switch Lifetime</b>
Uncoated Switch	$1 \times 10^4$ pulses
Diamond coating at anode	$4 \times 10^4$ pulses
Diamond coating at cathode	$1 \times 10^5$ pulses
Diamond coatings at both anode and cathode	$3 \times 10^5$ pulses

The schematic drawing of the switch damage for the test conditions of Table 2 is presented in Fig. 18. The switch gap is shown by the two horizontal lines of damage located at the front and the back of the switch corresponding to the limit of the copper plate electrodes. For comparison the negative photographs of the switch electrode areas after  $10^4$  shots are also shown in Fig. 18. The appearance of damage is consistent with the results of the switch lifetime tests presented in Table 2. It appears that the damage at the electrode contact areas eventually caused thermal runaway at the switch gap surface and produced a crack that shorted the gap. In experiments where the switch had no diamond coating, the majority of the time, a single current filament commutated the switches. The filament was initiated near the cathode and followed, approximately, one of the laser beams to the anode. Multiple branching as shown in Fig. 4 was rarely seen. In the case of the switch with diamond coating, the multiple branching was observed more often, indicating an increase of pre-avalanche sites.

As described earlier in this report, there is a rapid current increase in forward direction of an amorphous diamond/GaAs heterojunction where the diamond coating is biased negative with respect to the GaAs substrate. This case is schematically presented in Fig. 19 for the switch/electrode in an opposed configuration. In this case only the switch cathode was coated with a strip of thin film amorphous diamond.

As indicated in Table 2, the diamond coating of the switch anode area has resulted in increased hold-off characteristics of the PCSS in the off-state stage of operation leading to longer switch lifetimes. In this case the amorphous diamond inhibits the flow of electrons at the interface until very high fields are reached. This is due to rectifying behavior of the amorphous diamond/GaAs heterojunction operating under reverse bias condition as discussed earlier in this report.

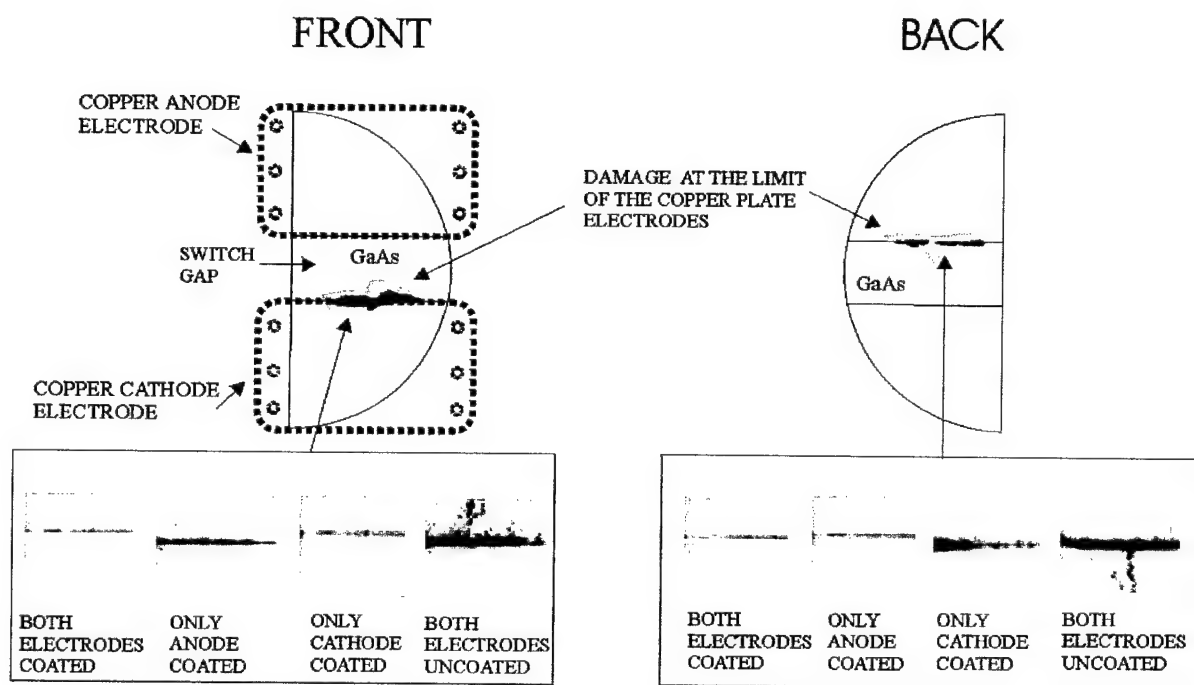


**Figure 18.** Schematic drawing of the appearance of damage on both sides of switch used in these studies. For comparison the negative photographs of the switch electrode areas for diamond-coated and uncoated switches are shown after  $1 \times 10^4$  commutation cycles.

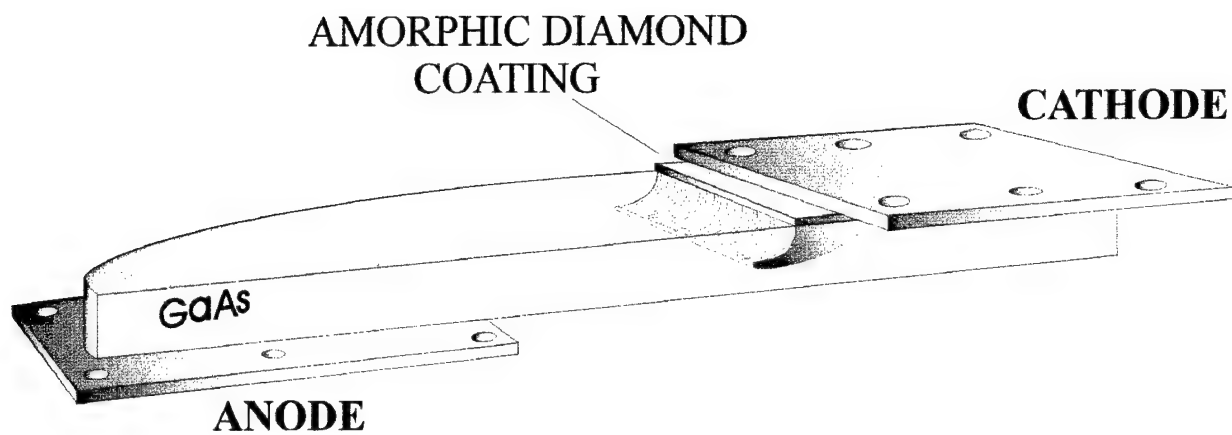


**Figure 19.** Schematic presentation of the switch/electrode assembly in an opposed configuration showing the off-state carrier movement due to the tunneling of electrons from amorphic diamond to GaAs.

## CONCLUSIONS

During this research program, a substantial effort was directed to study and implement the broadening of the current channels in the avalanche photoconductive switch in order to improve lifetime and increase switching peak power. Our main efforts were concentrated to study and use of amorphous diamond coatings at the switch electrodes to enhance operation and lifetime of a PCSS in stacked Blumlein pulse generators.

Enhancing or restricting the current conduction flow at the interface between amorphous diamond and PCSS material has pronounced effect upon the off-state switch hold-off and switch performance. For example, the tunneling of electrons from amorphous diamond to GaAs during the off-state stage of PCSS operation provides pre-avalanche sites that may diffuse conduction current upon switch activation. However, this may also increase leakage current at high fields causing switch shorting and failure. To avoid such problems for a particular charging voltage, it may be necessary to limit the current injection by controlling the switch gap, diamond film thickness.

Diamond coating of the switch anode area has resulted in increased hold-off characteristics of the PCSS in the off-state stage of operation leading to longer switch lifetimes. In this case the amorphous diamond restricted the flow of electrons at the interface until very high fields were reached. This is due to rectifying behavior of the amorphous diamond/ GaAs heterojunction operating under reverse bias condition as discussed earlier in this report.

In this work, the mechanical and semiconductor properties of amorphous diamond have been employed to improve the PCSS longevity by coating the switch cathode or anode areas or both. In order to further improve switch lifetime, the critical issue to resolve is the switch design options that make optimal use of amorphous diamond coatings for long life operations of

avalanche PCSS in stacked Blumlein pulsers. Design options include: switch configuration, switch gap setting, diamond film thickness, exact locations of diamond coatings and film qualities.

In this work, we studied the use of amorphous diamond film as photoconductive switch coating to improve the longevity and operation of PCSS devices in stacked Blumlein pulsers. Switch longevity was examined by fabrication and testing the PCSS treated with amorphous diamond under different switch design options such as switch configuration, switch gap setting, and diamond film thickness. A high power switch lifetime of  $3 \times 10^5$  cycles of commutation was realized by testing the diamond-coated switch performance in a prototype pulser. This presented a factor of 30 improvement in switch lifetime with application of amorphous diamond. It was shown that not only the diamond coating protected and hardened the cathode and anode sides but it also helped branching the filaments conducting high currents. We also studied the elementary processes involved in conduction of PCSS devices coated with amorphous diamond.

In addition to our own effort using amorphous diamond, there are other research programs in direction of improving PCSS lifetime in pulsed power systems. The longevity of the PCSS in pulsed power applications has been improved by doping the semi-insulating GaAs underneath the metal contacts [35]. Other efforts have focused on an opposed-contact PCSS with an  $n^+$  region next to the cathode electrode. Increased hold-off characteristic of this class of devices has been analyzed by simulation and it is shown that the introduction of the  $n^+$  region inhibits the flow of electrons at the interface until very high fields are reached [36]. Photoconductive switch enhancements realized in this work are well complementary and strengthen these efforts by utilizing unique semiconductor properties of amorphous diamond.

## EXECUTIVE SUMMARY

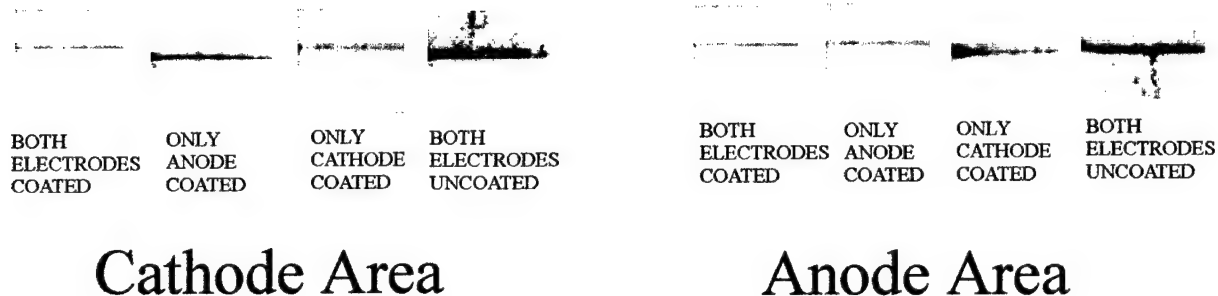
### 1. Summary of the Results

The principle goal of the research conducted under this grant was to develop a technology in pulsed power that could increase the voltage delivered to UWB antennas with reasonable switch lifetimes. During this program the Blumlein technology base and the level of understanding concerning the optimal use of capabilities of the Photoconductive Semiconductor Switches (PCSS) were significantly enlarged. Experiments with the stacked Blumlein prototype pulsers were conducted under different conditions of operation at power levels bypassing 100 MW. Special attention was placed on broadening of the current channels in the avalanche photoconductive switch in order to improve PCSS lifetime. The following Table presents the best simultaneous and individual results obtained, to date, by switching the stacked Blumlein pulsers with a high gain GaAs photoconductive semiconductor switch (PCSS).

Parameters	Simultaneous Results		Individual Results
Switch Voltage	60 kV	30 kV	100 kV
Switch Current	1.2 kA	0.6 kA	2 kA
Pulse Risetime	200 ps	200 ps	150 ps
R-M-S Jitter	500 ps	500 ps	200 ps
Optical Trigger Energy	300 nJ	300 nJ	300 nJ
Repetition Rate	10 Hz	20 Hz	200 Hz
Electric Field	60 kV/cm	60 kV/cm	100 kV/cm
Stack Voltage	112 kV	57 kV	175 kV
Switch Lifetime	$1 \times 10^4$ pulses	$3 \times 10^5$ pulses	$1 \times 10^6$ pulses

The mechanical and semiconductor properties of amorphous diamond were employed to improve the PCSS longevity by coating the switch cathode or anode areas or both. Issues concerning the switch longevity were studied by fabrication and testing the GaAs PCSS treated with the amorphous diamond under different switch configuration, gap settings, and diamond coating thickness. When the switch cathode was coated, the tunneling of electrons from amorphous diamond to GaAs provided pre-avalanche sites that diffused conduction current upon switch activation. On the other hand, the diamond coating of the switch anode resulted in increased hold-off characteristics and longer switch lifetimes by blocking leakage current during off-state stage of operation. A significant improvement in switch lifetime (a factor of 30) was demonstrated by coating the cathode and anode areas of a GaAs PCSS with amorphous diamond and testing its performance in a high power operation with a prototype stacked Blumlein pulser. Results of the switch lifetime tests by the application of amorphous diamond coating are given in the Table below. For comparison the negative photographs of the switch electrode areas for diamond-coated and uncoated switches for the test conditions stated in the Table are also shown after  $1 \times 10^4$  commutation cycles.

Test Condition	Switch Lifetime
Uncoated Switch	$1 \times 10^4$ pulses
Diamond coating at anode	$4 \times 10^4$ pulses
Diamond coating at cathode	$1 \times 10^5$ pulses
Diamond coatings at both anode and cathode	$3 \times 10^5$ pulses



In addition, during this work, elementary processes involved in conduction of diamond treated GaAs PCSS were extensively examined and possibilities for low power applications of heterojunction devices formed by amorphous diamond were given.

## 2. Personnel Participated

The professional personnel participated in the research program are listed below:

- |                     |                    |
|---------------------|--------------------|
| 1) Carl B. Collins  | Professor          |
| 2) Farzin Davanloo  | Research Scientist |
| 3) Mugurel C. Iosif | Graduate Student   |
| 4) Tiberius Camase  | Graduate Student   |

## 3. Publications Resulted from this Work

"Amorphous Diamond / Silicon Semiconductor Heterojunctions Exhibiting Photoconductive Characteristics," F. Davanloo, C. B. Collins, K.J. Koivusaari, and S. Leppävuori, Appl. Phys Lett., 77, 1837-1839 (2000).



"Photoconductive Switch Enhancements and Lifetime Studies for Use in Stacked Blumlein Pulsers," F. Davanloo, R. Dussart, K. J. Koivusaari, C. B. Collins and F. J. Agee, IEEE Trans. Plasma Sciences, 28, 1500-1506 (2000).

"Development of a Diamond Treated Photoconductive Semiconductor Switch for Use in Blumlein Pulsers," F. Davanloo, M.C. Iosif, D.T. Camase, C.B. Collins and F.J. Agee, Conference Record of the 2000 Twenty-Forth International Modulator Symposium, 2000, pp 73-77.

"High Power Photoconductive Semiconductor Switches Treated with Amorphous Diamond," F. Davanloo, M.C. Iosif, T. Camase, C.B. Collins and F.J. Agee, Proceedings of the Sixteenth International Conference on the Application of Accelerators in Research and Industry, Edited by J.L. Duggan and I.L. Morgan, AIP Conference Proceedings 576, 2001, pp 1047-1050.

"Development of High Power Photoconductive Semiconductor Switches Treated with Amorphous Diamond Coatings," F. Davanloo, M. C. Iosif, D. T. Camase, C.B. Collins, and F.J. Agee, Proceedings of the 13th International Pulsed Power Conference PPPS-2001, (IEEE, Inc. NJ, 2001), pp. 337-340.

"High Power Stacked Blumlein Pulsers Commutated by a Photoconductive Switch Treated with Amorphous Diamond," F.J. Agee, F. Davanloo, T. Camase, and C.B. Collins, Proceedings of SPIE Intense Microwave Pulses IX, H. E. Brandt, Editor, Vol. 4720, pp. 59-66 (2002).

"Progress in Development and Characterization of Photoconductively-Switched Stacked Blumlein Devices Producing High Power Nanosecond Pulses," F. Davanloo, C. B. Collins, and F. J. Agee, Proceedings of the 6<sup>th</sup> Ultra-Wideband Short – Pulse Electromagnetics Conference (UWB SP6), Annapolis, Maryland 3-7 June 2002 (accepted and pending for publication).

"Development of Photoconductive Switches for Stacked Blumlein Pulsers," F. Davanloo, C. B. Collins and F. J. Agee, Proceedings of the 14<sup>th</sup> International Conference on High Power Particle Beams, Beams 2002, Edited by T. A. Mehlhorn and M. A. Sweeney, AIP Conference Proceedings 650, 2002, pp. 91-94.

"Development and Characterization of Diamond Coated Photoconductive Switches for Stacked Blumlein Pulsers," F. Davanloo, C. B. Collins and F. J. Agee, Conference Record of the 2002 International Power Modulator Conference, (IEEE, Inc. NJ, 2002), pp. 187-190.

"Flash X-ray Sources powered by Blumlein Pulsers: Review and Prospect for X-rays with 100-ps Switching," F. Davanloo, C. B. Collins and F. J. Agee, Proceedings of SPIE 47<sup>th</sup> Annual International Symposium on Optical Science and Technology – Penetrating Radiation Systems and Applications IV, H. B. Barber, H. Roehrig, F. P. Doty, L. J. Porter, and E. J. Morton, Editors, Vol. 4786, PP. 162-172 (2002).

"Design, Fabrication and Performance of a Diamond Treated High Power Photoconductive Switch," F. Davanloo, C. B. Collins and F. J. Agee, Proceedings of the Seventeenth International Conference on the Application of Accelerators in Research and Industry, CAARI 2002, Edited by J.L. Duggan and I.L. Morgan, AIP Conference Proceedings (accepted and pending for publication).

"Mechanical and Semiconductor Properties of Nanophase Amorphous Diamond Coatings for High Power Electronics," F. Davanloo, C. B. Collins and F. J. Agee, Nanotech 2003, Volume 3, Technical Proceedings of the 2003 Nanotechnology Conference and Trade Show, (Computational Publications, Cambridge, 2003), pp. 350-353.

F. Davanloo, C. B. Collins, and F. J. Agee, "High Power Photoconductive Semiconductor Switches Treated with Amorphous Diamond Coatings," IEEE Transactions in Plasma Sciences, Vol. 30, No. 5, 1897-1904 (2002).

## **RESEARCH SIGNIFICANCE AND POTENTIAL APPLICATIONS**

During last few years new areas of pulsed power application have been introduced for the field of Bioelectrics [37]. These include biofouling prevention, bacterial decontamination, and medical applications such as electrochemotherapy and gene therapy. These applications are usually classified as outer membrane bioelectric effects [38]. Very recently, a major discovery was reported by Schoenbach, et al [39] where initial approaches to apply pulsed electric fields to kill cells by apoptosis were investigated. There, it was demonstrated as the applied pulse duration decreases from 300 ns to 10 ns, electric field effects are reduced at the level of the plasma membrane and are focused to the cell interior. If the electric field intensity is high enough apoptosis can be induced as indicated by the reduced size of treated mouse tumors [39]. This type of field-cell interaction using nanosecond pulses with high electric field has potential to affect transport processes across sub-cellular membranes and may be used for gene transfer into cell nuclei [38]. It can also trigger intracellular processes that can be used for cancer treatment by programmed cell death.

The intracellular electromanipulation processes require the development of reliable pulsed power sources that produce electric fields larger than 50 kV/cm at pulse durations into nanosecond

range [36]. In addition, the relatively low impedance of biological loads requires the characteristic impedance of the pulse generator to be around  $10\ \Omega$  [40]. Photoconductively-switched Blumlein pulse generators characterized during this AFOSR program are most suitable for the intracellular electromanipulations applications in the Bioelectric field because they have low inductance geometry that permits generation of ultra fast nanosecond waveforms easily matched and delivered to the biological loads.

Advances in stacked Blumlein technology for voltage multiplication at UTD, including progress made during this reporting period, also offer exciting possibilities for a variety of UWB applications especially in array UWB and compact UWB sources. Some of these sources are being used for synthetic aperture radar applications that inherently use the frequency content of pulses. At the 100 MW level of power, broad-band sources operating at kiloHertz repetition rates can be conceived that simply match compact pulsed power devices to the radiation impedance of free space.

It should be noted that the utilization of pulse power technology to treat cancer in human subjects ultimately requires non-intrusive methods such as UWB transmitters. Such devices could be used to provide necessary electric field strengths and durations at a tumor location in human body to promote apoptosis and cancer treatment. Sources employing UWB schemes feature fast rising short pulse width waveforms with broad frequency contents that are suitable for intracellular electromanipulations.

The development of UWB sources has been pursued in two general directions. The first uses a single pulser to feed a very high voltage to a single antenna transmitter. The pulser can be used to feed a non-dispersive high gain antenna system to achieve high field strength in the far field of the antenna. The second approach employs many radiating elements (array UWB

source) switched at relatively low voltage to collectively deliver an additive field at the target of the array. The photoconductive semiconductor switched (PCSS) array method has been employed and demonstrated in the systems such as GEM series of pulsers at the U.S. Air Force Research Laboratory [41]. The stacked Blumlein technology and amorphous diamond coating offer tremendous advantage for pulser development for such UWB schemes that can provide non-intrusive probe of human body for medical treatments if suitable electric strength and pulse parameters are identified. Ongoing progress made in stacked Blumlein technology also offers significant advantage for the array source concept by reliable delivery of higher voltages to each radiating element than that available with existing photoconductively -switched systems.

Another of the new application currently opening involves the modulation of nuclear properties. Of particular interest are nuclear spin isomers. They store the highest densities of energy possible without nuclear reactions. For example, an isomer of  $^{178}\text{Hf}$  stores 2.445 MeV per atom for a shelf life of 31 years [42]. In practical terms this means that a sample of the size of a golf ball would store the energy equal to 10 tons of chemical fuels or explosives. However, in nuclear spin isomers the energy is stored electromagnetically so that it would be released as x-rays and  $\gamma$ -rays, if it could be triggered. Progress made in Blumlein technology during our current AFOSR Program offer a unique opportunity to develop flash x-ray capabilities with 100 ps switching. Since the maximum x-ray dose is emitted before the discharge diode current rises to its peak, such table-top device is expected to produce high power repetitive x-ray pulses into below ns range with risetimes on the order of 100 ps. This device could provide non-thermal x-ray illumination of extended isomer absorbers with yields above  $10^{20}$  keV/keV in a short operating time.

The results of studies performed in this work should guide the reliable use of compact pulse power sources commuted with photoconductive switches that can provide subnanosecond

high power pulses at kHz repetition rates. Examples of applications that are of interest to civilian sector include: Bioelectrics, microwave dewaxing of casting molds, microwave oil sludge separation, ozone treatment, and selective bond-breaking for destroying toxic materials. The pulse power systems being developed in this work can also be used to commutate a new generation of flash x-ray devices and laser systems capable of generating high power nanosecond pulses.

### REFERENCES

1. F. Davanloo, J. D. Bhawalkar, C. B. Collins, F. J. Agee, and L. E. Kingsley, "High Power, Repetitive Stacked Blumlein Pulse Generators Commuted by a Single Switching Element," *Conference Record of the 1992 Twentieth Power Modulator Symposium*, pp. 364-367, IEEE, Piscataway, 1992.
2. J. D. Bhawalkar, F. Davanloo, C. B. Collins, F. J. Agee, and L. E. Kingsley, "High Power Repetitive Stacked Blumlein Pulse Generators Producing Waveforms with Pulse Durations Exceeding 500 nsec," *Proceedings of the 9th International Pulsed Power Conference*, pp. 857-860, IEEE, Piscataway, 1993.
3. J. D. Bhawalkar, D. L. Borovina, F. Davanloo, C. B. Collins, F. J. Agee, and L. E. Kingsley, "High Power Repetitive Stacked Blumlein Pulse Generators," *Proceedings of the International Conference on Lasers '93*, V. J. Corcoran and T. A. Goldman, Eds., pp. 712-717, STS Press, Mclean, 1994.
4. F. Davanloo, D. L. Borovina, J. D. Bhawalkar, C. B. Collins, F. J. Agee, and L. E. Kingsley, "High Power Repetitive Waveforms Generated by Compact Stacked Blumlein Pulsers," *Conference Record of the 1994 Twenty-First Power Modulator Symposium*, pp. 201-205, IEEE, Piscataway, 1994.
5. F. Davanloo, C. B. Collins, and F. J. Agee, "High power, repetitive-stacked Blumlein pulsed commutated by a single switching element," *IEEE Trans. Plasma Sciences*, **26**, pp. 1463-1475, 1998.
6. F. Davanloo, D. L. Borovina, J. L. Koriath, R. K. Krause, C. B. Collins, F. J. Agee, J. P. Hull, J. S. H. Schoenberg and L. E. Kingsley, in: *Ultra-Wide-Band, Short-Pulse Electromagnetics 3*, edited by C. E. Baum, L. Carin and A. P. Stone (Plenum Press, New York, 1997) pp. 31-38.
7. F. Davanloo, R. Dussart, M. C. Iosif, C. B. Collins and F. J. Agee, "Photoconductive Switch Enhancements and Lifetime Studies for Use in Stacked Blumlein Pulsers,"

*Proceedings of the 12th International Pulsed Power Conference*, C. Stallings and H. Kirbie, Eds., pp. 320-323, IEEE, Piscataway 1999.

8. F. J. Agee, Current Issues in High Power Microwaves, in: *Conference Record of the 1996 Twenty-Second Power Modulator Symposium* (IEEE, Piscataway, 1996) pp. 1-4.
9. C. B. Collins, F. Davanloo, and T. S. Bowen, "Flash x-ray source of intense nanosecond pulses produced at high repetition rates," *Rev. Sci. Instrum.* **57**, pp. 863-865, 1986.
10. F. Davanloo, T. S. Bowen, and C. B. Collins, "Scaling to high average powers of a flash x-ray source producing nanosecond pulses," *Rev. Sci. Instrum.* **58**, pp. 2103-2109, 1987.
11. F. Davanloo, J. J. Coogan, T. S. Bowen, R. K. Krause, and C. B. Collins, "Flash x-ray source excited by stacked Blumlein generators," *Rev. Sci. Instrum.* **61**, pp. 1448-1456, 1990.
12. J. J. Coogan, F. Davanloo, and C. B. Collins, "Production of high energy photons from flash x-ray sources powered by stacked Blumlein generators," *Rev. Sci. Instrum.* **59**, pp. 2260-2264, 1988.
13. F. J. Zutavern, G. M. Loubriel, W. D. Helgeson, M. W. O'Malley, R. R. Gallegos, A. G. Baca, T. A. Plut, and H. P. Hjalmarson, Fiber-optic Control of Current Filaments in High Gain Photoconductive Semiconductor Switches, in: *Conference Record of the 1994 Twenty-First Power Modulator Symposium* (IEEE, Piscataway, 1994) pp. 116-119.
14. F. Davanloo, E. M. Juengerman, D. R. Jander, T. J. Lee, and C. B. Collins, "Amorphous diamond films produced by a laser plasma source," *J. Appl. Phys.*, vol. 67, pp. 2081-2087, 1990.
15. F. Davanloo, E. M. Juengerman, D. R. Jander, T. J. Lee, and C. B. Collins, "Laser plasma diamond," *J. Mater. Res.*, vol. 5, pp. 2398-2404, 1990.
16. F. Davanloo, T. J. Lee, D. R. Jander, H. Park, J. H. You, and C. B. Collins, "Adhesion and mechanical properties of amorphous diamond prepared by a laser plasma source," *J. Appl. Phys.*, **71**, 1446-1453, 1992.
17. C. B. Collins, F. Davanloo, J. H. You, and H. Park, "Nanophase diamond films produced by laser deposition," in *Proc. SPIE Laser Application*, vol. 2097, 1994, p.129.
18. C. B. Collins, F. Davanloo, T. J. Lee, H. Park, and J. H. You, "Noncrystalline films with the chemistry, bonding, and properties of diamond," *J. Vac. Sci & Technol B*, vol. 11, pp. 1936-1941, 1993.
19. F. Davanloo, H. Park and C.B. Collins, "Protective coating of nanophase diamond deposited directly on stainless steel substrates," *J. Mat. Res.*, vol. 11, pp. 2042-2050, 1996.

20. F. Davanloo, C. B. Collins, and K. J. Koivusaari, "Scratch adhesion testing of nanophase diamond coatings on steel and carbide substrates," *J. Mater. Res.*, vol. 14, pp. 3474-3482, 1999.
21. F. Davanloo, C. B. Collins and K. J. Koivusaari, "Scratch adhesion testing of nanophase diamond coating on industrial substrates," in *Adhesion Measurements of Films & Coatings*, vol. 2, K.L. Mittal, Ed., Netherlands: VSP, 2001, pp. 141-157.
22. C. B. Collins, F. Davanloo, D. R. Jander, T. J. Lee, H. Park and J. H. You, "Microstructure of amorphous diamond films," *J. Appl. Phys.*, vol. 69, pp. 7862-7870, 1991.
23. N. Konofaos, and C. B. Thomas, "Characterization of heterojunction devices constructed by amorphous diamondlike films on silicon," *J. Appl. Phys.*, vol. 81, pp. 6238-6245, 1997.
24. V. S. Veerasamy, G. A. J. Amaratunga, J. S. Park, H. S. MacKenzie and W. I. Milne, "Properties of n-type tetrahedral amorphous carbon (ta-C)/p-type crystalline silicon heterojunction diodes," *IEEE Trans. Electron Devices*, vol. 42, pp. 577-585, 1995.
25. V. S. Veerasamy, G. A. J. Amaratunga, J. S. Park, W. I. Milne, H. S. MacKenzie and, D. R. McKenzie, "Photoresponse characteristics of n-type tetrahedral amorphous carbon/p-type Si heterojunction diodes," *Appl. Phys. Lett.*, vol. 64, pp. 2297-2299, 1994.
26. L. K. Cheah, X. Shi, E. Liu and J. R. Shi, "Nitrogenated tetrahedral amorphous carbon films prepared by ion-beam-assisted filtered cathodic vacuum arc technique for solar application," *Appl. Phys. Lett.*, vol. 73, pp. 2473-2475, 1998.
27. J. Mort and K. Okumura, "Photosensitization of diamond thin films," *Appl. Phys. Lett.*, vol. 56, pp. 1898-1900, 1990.
28. F. Davanloo, R. Dussart, K.J. Koivusaari, C.B. Collins, and F.J. Agee, "Photoconductive Switch Enhancements and Lifetime Studies for Use in Stacked Blumlein Pulsers," *IEEE Trans. Plasma Sciences*, **28**, pp. 1500-1506, 2000.
29. F. Davanloo, M. C. Iosif, D. T. Camase, C. B. Collins and F. J. Agee, "Development of a diamond treated photoconductive semiconductor switch for use in Blumlein pulsers," in *Conference Record of the 2000 Twenty-Forth International Modulator Symposium*, 2000, pp. 73-77.
30. F. Davanloo, M. C. Iosif, T. Camase, C. B. Collins and F. J. Agee, "High power photoconductive semiconductor switches treated with amorphous diamond coatings," edited by J. L. Duggan and I. L. Morgan, *AIP Conference Proceedings 576*, New York, 2001, pp. 1047-1050.



31. F. Davanloo, C. B. Collins, K. J. Koivusaari and S. Leppävuori, "Amorphous diamond/silicon semiconductor heterojunctions exhibiting photoconductive characters," *Appl. Phys. Lett.*, vol. 77, pp. 1837-1839, 2000.
32. E.D. Hinkle, R.H. Rediker, and D.K. Jadus, *Appl. Phys. Lett.* 6, 144 (1965).
33. G.H. Dohler and M.H. Brodsky, "Amorphous-Heterojunctions", AIP Conference Proceedings No. 20, (Yorktown Heights, 1974), pp.351-356.
34. J.P. Donnelly and A.G. Milnes, "current/voltage characteristics of p- n Ge-Si and Ge-GaAs heterojunctions", *Proceedings IEEE* 113, 1468 (1966).
35. A. Mar, G. M. Loubriel, F. J. Zutavern, M. W. O'Malley, W. D. Helgeson, D. J. Brown, H. P. Hjalmarson, A. G. Baca, R. L. Thornton, and R. D. Donaldson , "Longevity Improvement of Optically Activated, High Gain GaAs Photoconductive Semiconductor Switches", in Conference Record of the 2000 Twenty-Forth International Modulator Symposium, 2000, p. 69-72.
36. N. Islam, E. Schamiloglu, C. B. Fleddermann, J. S. H. Schoenberg, and R. P. Joshi, "Improved Hold-Off Characteristics of GaAs Photoconductive Switches Used in High Power Applications", in *Proceedings of the 12th International Pulsed Power Conference*, pp. 316-319, 1999.
37. C. Polk, "Biological applications of large electric fields: Some history and fundamentals, *IEEE Trans. Plasma Sciences* **28**, pp. 6-14, 2000.
38. K. H. Schoenbach, S. Katsuki, R. H. Stark, E. S. Buescher and S. J. Beebe, "Bioelectrics-New applications for pulsed power technology," *IEEE Trans. Plasma Sciences* **30**, pp. 293-301, 2002.
39. S. J. Beebe, P. M. Fox, L. J. Rec, K. Somers, R. H. Stark, and K. H. Schoenbach, "Nanosecond pulsed electric field (nsPEF) effects on cell and tissues: Apoptosis induction and tumor growth inhibition," *IEEE Trans. Plasma Sciences* **30**, pp. 286-292, 2002.
40. J. Deng, R. H. Stark and K. H. Schoenbach, "A Compact, Nanosecond Pulse Generator with Water as Dielectric and as Switch Medium, *Proceedings of the 13th International Pulsed Power Conference PPPS-2001*, pp. 1587-1590, IEEE, Piscataway, 2002.
41. F. J. Agee, D. W. Scholfield, W. Prather and J. W. Burger, "Powerful Ultra-Wide Band Emitters: Status and Challenges," *Proc. SPIE* 2557, pp. 98-106, 1995.
42. C. B. Collins, N. C. Zoita, A. C. Rusu, M. C. Iosif, D. T. Camase, F. Davanloo, S. Emura, T. Uruga, R. Dussart, J. M. Pouvesle, C. A. Ur, I. I. Popescu, V. I. Kirischuk, N. V. Strilchuk, and F. J. Agee, "Tunable synchrotron radiation used to induce gamma-emission from the 31 year isomer of  $^{178}\text{Hf}$ ," *Europhys. Lett.*, **57**, pp. 677-682, 2002.